ARMY RESEARCH LABORATORY

The Four-Dimensional Fire-Induced Transmittance and Turbulence Effects Model: FITTE

by Dorothy Bruce
Battlefield Environment Directorate

19960327 051

Approved for public release; distribution is unlimited.

DTIC QUALITY INSPECTED 1

NOTICES

Disclaimers

REPORT DOCUMENTATION PAGE

Form Approved
OMB No. 0704-0188

1. AGENCY USE ONLY (Leave blank)	2. REPORT DATE August 1995	3. REPORT TYPE AND DATES COVERED Final

4. TITLE AND SUBTITLE

The Four-Dimensional Fire-Induced Transmittance and Turbulence Effects Module: FITTE

5. FUNDING NUMBERS

6. AUTHOR(S)

Dorothy Bruce

7. PERFORMING ORGANIZATION NAME(S) AND ADDRESS(ES)

U.S. Army Research Laboratory
Battlefield Environment Directorate
Attn: AMSRL-BE-S
White Sands Missile Range, NM 88002-5501

8. PERFORMING ORGANIZATION REPORT NUMBER

ARL-TR-273-6

9. SPONSORING/MONITORING AGENCY NAME(S) AND ADDRESS(ES)

U.S. Army Research Laboratory
2800 Powder Mill Road
Adelphi, MD 20783-1145

10. SPONSORING/MONITORING AGENCY REPORT NUMBER

ARL-TR-273-6

11. SUPPLEMENTARY NOTES

12a. DISTRIBUTION/AVAILABILITY STATEMENT

Approved for public release; distribution is unlimited.

12b. DISTRIBUTION CODE

A

13. ABSTRACT (Maximum 200 words)

The four-dimensional fire-induced transmittance and turbulence effects module (FITTE) calculates transmittance and laser beam spread and wander for propagation paths through battlefield vehicular or hydrocarbon fires and also calculates radiance from the fire and/or fire plume. It can perform the transmittance and radiance calculations for a rectangular array of points and create an output file which can be used to add images of battlefield fires into scenes.

This document contains both a technical description of the model and a user's guide.

14. SUBJECT TERMS

fire, transmittance, turbulence effects, radiance, beam wander, beam spread, emissive sources

15. NUMBER OF PAGES

126

16. PRICE CODE

17. SECURITY CLASSIFICATION OF REPORT	18. SECURITY CLASSIFICATION OF THIS PAGE	19. SECURITY CLASSIFICATION OF ABSTRACT	20. LIMITATION OF ABSTRACT
Unclassified	Unclassified	Unclassified	SAR

Acknowledgments

Contents

Figures

4

Appendix Figures

Tables

Appendix Table

6

1. Introduction

The Fire-Induced Transmission and Turbulence Effects (FITTE) module predicts transmittance through fire plumes, emitted radiance from fires and fire plumes, and, optionally, effects of fire and fire plume turbulence on laser propagation for a given line of sight (LOS). The FGLOW model option extends the calculations to multiple LOSs to predict the radiant image of a fire or fire plume segment seen by an imaging system. The fires represent localized sources of burning diesel fuel, motor oil, and rubber (simulated burning vehicles). FITTE also predicts the path-integrated particulate concentration, and, if a target temperature is specified, the attenuated thermal radiance from the target at the observer position. If the calculation is performed for a single wavelength, the model predicts beam spread and wander for a laser beam of that wavelength.

The FGLOW option performs calculations for a fan-shaped rectangular set of LOSs. It creates a file of emitted radiance values, that represent the radiant image of the fire or fire plume seen by an imaging system, and of transmittance values that represent the attenuation of the background radiance. An option allows output of an apparent temperature image of the fire or fire plume.

The information in the technical manual (sections 1 through 3) describes the model at the time it was furnished to the Electro-Optical Systems Atmospheric Effects Library (EOSAEL). Changes at future dates will be documented in a README or similar text file, which should be distributed with the code. Similar comments apply to the user's manual (sections 4 and 5).

1.1 Names of Things

EOSAEL standard typefaces are used for descriptions:

1. Names of modules are in univers style.

2. Variable and subroutine names are in courier style.

3. Sample input and output are in typewriter style, monospaced to allow column alignment.

1.2 Availability

EOSAEL 92 is available at no cost to U.S. Government agencies, specified Allied organizations, and their authorized contractors. U.S. Government agencies needing EOSAEL 92 should send a letter of request, signed by a branch chief or division director, to U.S. Army Research Laboratory (ARL). Contractors should have their Government contract monitor send the letter of request. Allied organizations must request EOSAEL 92 through their national representative. The EOSAEL 92 point of contact at ARL is Dr. Alan Wetmore.

Include intended uses with requests. Also, include the type of nine-track tape necessary for computer execution. Tape formats are as follows: ASCII, UNIX tar format in 1600 or 6250 bpi, or SUN cartridge. EOSAEL 92 cannot be supplied on other media. Documentation for modules is included.

1.2.1 Mailing Address

Director
Battlefield Environment Directorate
Army Research Laboratory
AMSRL-BE-S (Attn: Dr. A. Wetmore)
White Sands Missile Range, NM 88002-5501

1.2.2 Phone and Electronic Mail

	(505) 678-5563
FAX	(505) 678-2432
DSN	258-5563
email	awetmore@arl.mil

2. Background

The FITTE/FGLOW model was developed to provide relatively rapid calculations of the effects of battlefield fires on detection, laser-designator, and weapon systems. Earlier versions of the models treated the fire and fire plume as static mean-value entities.

Although much work has been done on modeling laser propagation in the atmosphere, the situations modeled were those for which homogeneous, isotropic turbulence could be assumed. The assumptions permit simplifications in calculations of short- and long-time average spot size and average centroid jitter not valid for propagation through a fire plume.

Fire plumes are regions of space where there are rapidly changing atmospheric conditions. Special algorithms are needed to treat the effects of fire plume turbulence on propagation because of the rapid changes in refractive index within the plume, the large and nonuniform increase in the refractive index structure constant, and the fact that the turbulence effects depend on path-weighted turbulence parameters.

A preliminary model of the effects of a vertical fire plume on laser propagation was developed (Thompson and DeVore 1981) for the U.S. Army Atmospheric Sciences Laboratory (ASL). This model was modified (Bruce, Sutherland, and Larson 1982) to handle bent-over plumes with obscuration from smoke for EOSAEL 82. The model predicted transmittance through the plume for a given LOS and wavelength, and it optionally predicted magnitudes of beam wander and beam spread. The transmittance depended only on the plume aerosols because the major gaseous effluents, water vapor and carbon dioxide, are responsible for less than 5 percent of the total extinction in the visual and infrared (IR) atmospheric window regions of the spectrum where many Army systems operate.

Fire and plume parameters (fire temperature and plume vertical velocity) were obtained from laboratory and field measurements (D. Bruce, unpublished data; C. W. Bruce, private communication 1982). Smoke optical parameters were obtained by a semiempirical approach. A theoretical approach to determining specific extinction coefficients for carbonaceous aerosols has been described

9

(Chylek et al. 1981). This entails assuming equivalent spheres with appropriate particle-to-void ratios and applying Mie scattering theory. For the FITTE model, particle-to-void theory was modified to give agreement with transmissometer data (Sutherland and Walker 1982; Sutherland, Hoock, and Khanna 1984).

Minor changes were made in the FITTE model for EOSAEL 84. The changes, primarily, were to the calculation of radiative transfer. Model output was expanded to include attenuated target radiance from a hot target and emitted radiance from the plume, which made it possible to predict target contrast.

The Forschungsinstitut für Optik commissioned the development of the FEUER code (Manning 1985), which was a modification of the 1984 version of FITTE that added effects of absorption and emission by the major effluent gases to the predictions and the capability to perform calculations over a waveband. The work was based on a modification of code from the ATLES model (Young 1977). Temperature-dependent values of absorption coefficients are included for water vapor in the spectral region from 2.222 to 200.000 μm (4500 to 50 cm^{-1}), and for carbon dioxide in the regions from 2.702 to 3.225 μm (3700 to 3100 cm^{-1}) and 4.160 to 5.000 μm (2400 to 2000 cm^{-1}). Data are included for temperatures from 100 to 3000 K. The FEUER code was supplied to ASL for incorporation into the EOSAEL 87 version of FITTE.

The FGLOW model (Bruce 1988) also was added for EOSAEL 87. FGLOW is an extension of FITTE that performs transmittance and emitted radiance calculations for a set of LOSs in a fan-shaped rectangular array. The output can be used to predict the mean image of the fire or fire plume that would be seen by an imaging sensor, or it may be used in conjunction with an appropriate algorithm to add a fire plume to a background image.

Significant changes were made for the first revision of EOSAEL 87 FITTE. Some changes result from work done (to increase the speed of calculation) for the Forschungsinstitut für Optik by OptiMetrics, Inc. (Manning and Kebschull 1988), and other changes result from work at ARL. Most of the changes are transparent to the user. They cause an increase in the speed of calculations by up to a factor of 10, particularly for waveband and FGLOW image calculations.

10

Time-dependent spatial variations were added to the FITTE/FGLOW model for EOSAEL 92. The variations were accomplished by adding time-dependent fluctuations to the centerline position and to most of the mean-value Gaussian-distributed parameters. Other changes include options to perform time-series calculations and to vary one or more of the fire parameters.

2.1 Conceptual Overview of FITTE

Simplified physical models of fires and fire plumes are combined with a model for radiative transfer to predict the effects of battlefield fire plumes on propagation of visual and IR radiation or to predict values needed to evaluate the effects of fire plumes on imaging sensors. A specially tailored model of the turbulence structure function within a fire plume is used to predict beam spread and wander for laser propagation. Empirical data and results of theoretical calculations are used for fire and aerosol parameters.

2.2 The Physical Models

2.2.1 The Fire and Fire Plume Models

The fire and fire plume are described in terms of mean time-averaged parameters with time-varying fluctuations superimposed to create dynamical variation. The description of the mean value model is given first. A description of the fluctuation modeling follows.

2.2.1.1 The Time-Averaged Fire.—FITTE/FGLOW uses an extremely simple model for the fire itself. A fire is modeled as a circular disk with fixed mean temperature T_o, radius R_o, and burn time t_{burn}, and specific quantities of fuel. Observational evidence shows that the burn time should be a function of windspeed, and such dependence may be incorporated into the model after quantitative data become available.

The fire is centered at the origin of the model coordinate system. The model coordinate system is a right-handed coordinate system with the positive x-axis coinciding with the downwind direction. The coordinate system is used because it affords the simplest possible equations. Transformation to and from other coordinate systems is done using standard EOSAEL conventions.

The user specifies a fire type from several types that represent burning vehicles or vehicular fuels. The model is restricted to these fires because they are the only type of fuel mixture for which a relatively complete set of data is available. The fire size is restricted so the fire does not significantly change the atmospheric parameters used in the calculations.

The fire characteristics were chosen based on data from Battlefield Induced Contamination Tests I and III (BICT I and BICT III) (Kennedy 1981; Kennedy 1982). The characteristics were designed to give realistic values for mean heat and aerosol fluxes. Types 1, 2, and 3 correspond roughly to small (jeep), medium (truck), and large (tank) burning vehicles, while type 4 is a larger fire that represents a small fuel depot. The four types should be reasonable representations of battlefield fires. Table 1 lists defining values for the fires.

Table 1. Values defining model fires

	Type	Diesel Fuel		Motor Oil		Rubber	Radius
		(gal)	[kg]	(qt)	[kg]	(kg)	(m)
Jeep	1	5	[16.821]	6	[5.0463]	40	0.6
Truck	2	20	[67.284]	8	[6.7284]	100	1.0
Tank	3	125	[420.525]	16	[13.4568]	250	2.0
Fuel Depot	4	800	[2,691.360]	160	[134.5680]	0	4.0

Quantities derived from the source parameter values are the aerosol (smoke) mass emission rate, the heat emission rate, and the number densities of the major molecular combustion products (carbon dioxide and water vapor). The values are converted to fluxes through the plume cross-sectional area.

Calculation of the aerosol mass emission rate Q_M requires a value for the particulate emission factor E_f, the ratio of the mass of particulates produced to the mass of fuel consumed in the combustion process. This quantity is difficult to determine and is estimated from experimental data (Sutherland and Walker 1982) to be 0.160 g/g. The mass emission rate is modeled as

$$Q_M = E_f \frac{M_{DF} + M_{MO} + M_{RU}}{t_{burn}} \tag{1}$$

where M is the total mass (in grams) of diesel fuel (DF), motor oil (MO), or rubber (RU), and t_{burn} is the total burn time, set to 25 min to obtain heat and mass flux levels similar to those at the BICT tests.

The heat emission rate Q_H is given by

$$Q_H = (1 - E_f) \frac{E_{DF} M_{DF} + E_{MO} M_{MO} + E_{RU} M_{RU}}{t_{burn}} \tag{2}$$

where the E's in the numerator are the heat of combustion of the various fuels.

The factor $(1 - E_f)$ arises to account for the fact that particulates are unburned residue of the combustion process. Values for the heats of combustion are summarized (Gomez et al. 1980) from data (Turner, Eitner, and Manning 1980; Levitt and Levitt 1982).

The molecular concentrations (number of molecules/cc) of the major combustion products are arrived at as follows. Combustion of diesel fuel is represented (Leslie et al. 1980) by

$$2\ CH_{1.8} + 2.9\ O_2 + 10.93\ N_2 \rightarrow 2\ CO_2 + 1.8\ H_2O + 10.93\ N_2\ . \tag{3}$$
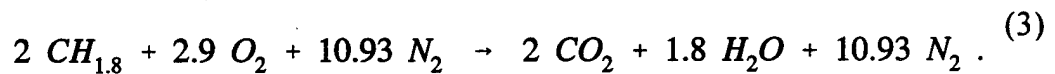
The reaction in equation (3) is a composite representation of a set of reactions, one for each of the various fuel molecules. Although the reaction in equation (3), generally, is used to approximate combustion in an engine, it is equally valid for combustion in air. The molecular concentration of carbon dioxide caused by combustion, C_{S1}, in a 1-cm high volume above a fire of area a_F cm^2 is

$$C_{SI} = \frac{hydrocarbon\ fuel\ weight}{molecular\ weight\ of\ CH_{1.8}} \cdot N_A \cdot \frac{1}{t_{burn}} \cdot \frac{1}{a_F \cdot s_o} \qquad (4)$$

where N_A is Avogadro's number and s_o is the effluent velocity (cm/s) just above the fire.

From equation (3), the molecular concentration of water vapor, C_{S2}, produced by combustion is 0.9 times that of carbon dioxide.

The mean temperature (923.16 K) for the top hat fire distribution was chosen based on unpublished data taken by the author during BICT I (Kennedy 1981). This translates to a peak temperature of roughly 2000 K for the equivalent Gaussian distribution used in the propagation model.

2.2.1.2 *The Time-Averaged Fire Plume.*—FITTE uses a top hat plume model to describe the transport of general curved plumes as well as the special cases of horizontal and vertical plumes. The top hat distribution has a single value within the plume radius and is zero outside the plume.

The two-thirds law model (Briggs 1969) is used to predict the time-averaged plume centerline. The plume centerline equation for a finite source at the origin of the coordinate system is

$$z + z_V = \frac{C}{U} (x + x_V)^{2/3} \qquad (5)$$

where x and z are plume centerline coordinates in the x-z plane, x_V and z_V are constant coordinates of a virtual point source and are chosen to match boundary conditions at the fire source, and U is the ambient mean windspeed (assumed uniform with height).

U is not permitted to be less than 0.10 m/s to ensure that equation (5) is well defined. Figure 1 shows a time-averaged plume in the model coordinate system.

14
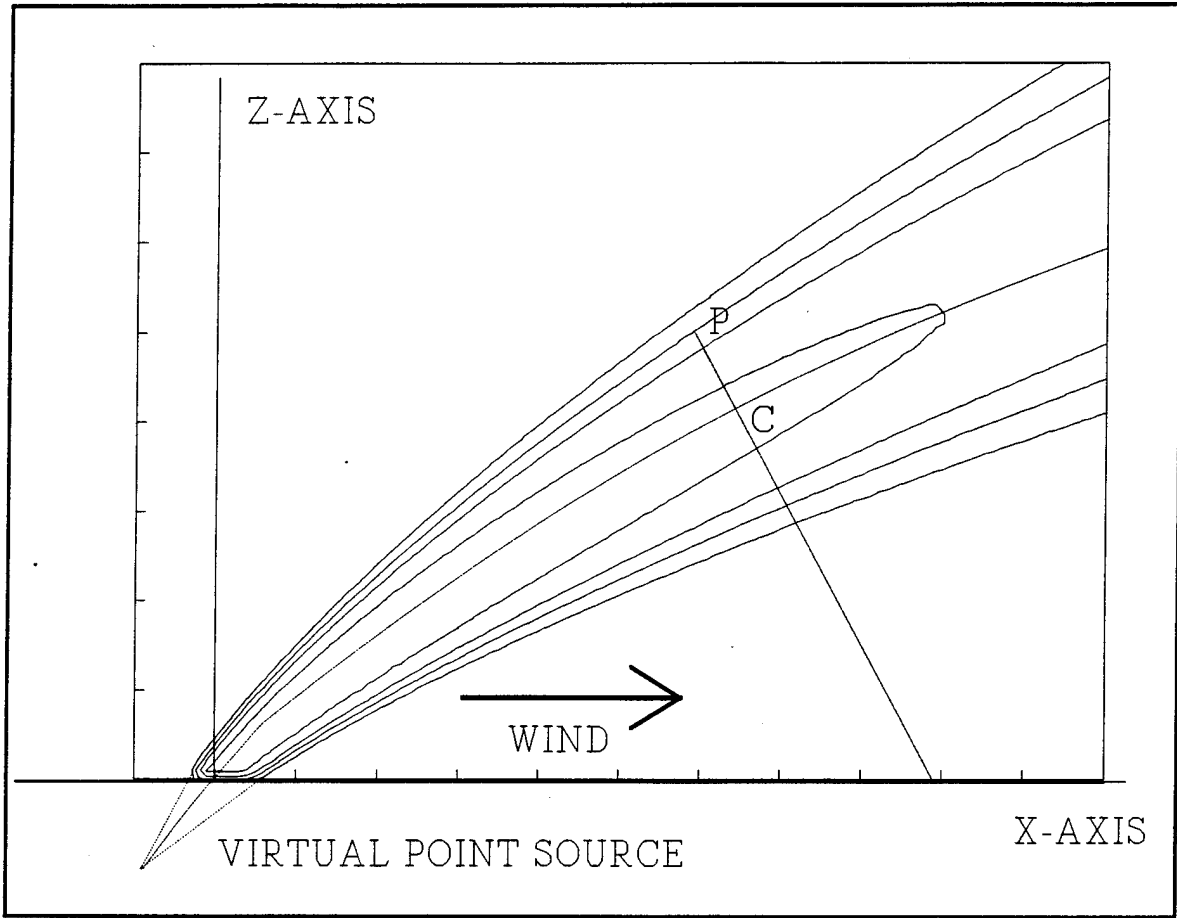
Figure 1. Side view contour plot of a fire plume in the model coordinate system. The plume edges shown are at the at the e^{-2} points of a conical Gaussian distribution. The centerline is sketched.

The constant C is given by (Weil 1981) as

$$C = \left(\frac{3F}{2\xi^2} \right)^{1/3} \tag{6}$$

where ξ is an entrainment constant; a constant that describes the fractional increase in plume volume per unit distance along the centerline caused by diffusion, and F is the buoyancy flux.

F is defined as

$$F = \frac{gQ_H}{\pi C_P \rho_A T_A} = g W_o R_o^2 \frac{(T_o - T_A)}{T_o} \tag{7}$$

where g is the gravitational acceleration, Q_H is the source heat flux, C_P is the specific heat of air at constant pressure, ρ_A is the ambient air density, T_A is the ambient temperature, T_o is the source temperature, W_o is the initial plume vertical velocity, and R_o is the source radius.

If it is assumed that the buoyancy flux is conserved, equation (7) applies at any height z if the values T_o, W_o, and R_o are replaced by $T(z)$, $W(z)$, and $R(z)$, respectively.

Using a geometrically based argument similar to those in the literature (Hoult, Fay, and Forney 1969), the entrainment parameter, ξ, for a general plume can be expressed as

$$\xi = \eta \left[1 - \left(\frac{U}{S} \right)^2 \right] + \upsilon \left(\frac{U}{S} \right)^2 \tag{8}$$

where η is the empirically determined entrainment constant for a vertical plume, υ is the empirically determined entrainment constant for a horizontal plume, and S is the plume velocity along the centerline.

Experimentally determined values used for entrainment into vertical and horizontal plumes are $\eta = 0.12$ and $\upsilon = 0.60$, respectively (Hoult and Weil 1972), although values have been reported (Briggs 1969) as low as 0.07 for vertical plumes and as high as 1.0 for horizontal plumes. ξ must be constant to maintain model simplicity, so the value of plume velocity at the origin $S(0)$ is used in the defining equation.

The mean velocity along the centerline S is assumed to be the vector sum of the ambient mean wind vector U and the mean vertical plume velocity W. S and W may be written as functions of z or, alternatively, in terms of D, the distance from the origin along the centerline. The time-averaged plume parameters, assumed to have Gaussian distributions about the plume centerline (George, Alpert, and Tamanini 1977), are most easily expressed as functions of D and of the plume width parameter $\sigma(D)$.

The relation between the value of the centerline coordinate z and the distance D of that point from the origin is obtained as follows. The ambient wind is assumed to be horizontal, so $W(z)$ can be expressed as

$$\frac{W(z)}{U} = \frac{(dz/dt)}{(dx/dt)} = \frac{dz}{dx} \qquad (9)$$

at any point on the centerline.

Substitution for dz/dx from the plume centerline equation gives

$$W(z) = \frac{2}{3} C^{3/2} \frac{1}{\sqrt{U(z + z_V)}} . \qquad (10)$$

Because the vertical wind velocity at the origin W_0 is known and ξ is defined in terms of known quantities, the constants z_V, x_V, and C can be found.

The plume model assumes that the time-averaged plume parameter distributions vary as functions of D. Therefore, it is usually more convenient to express the parameters as functions of D rather than of centerline height z. The relationship between D and z is found by integrating

$$dD = \sqrt{(dx/dz)^2 + 1} \ dz \qquad (11)$$

from the origin to the point of interest, z_{CI}, along the centerline.

Integrating equation (11) gives

$$D = \left(\frac{2C}{3U}\right)^3 \left[\sqrt[3/2]{(z_{CI} + z_V)\left(\frac{9}{4}\right)\left(\frac{U}{C}\right)^3 + 1} - \sqrt[3/2]{z_V\left(\frac{9}{4}\right)\left(\frac{U}{C}\right)^3 + 1} \right] . \qquad (12)$$

2.2.1.3   *Time-Averaged Distribution Functions.*—Spatially resolved measurements of time-averaged plume parameters, such as temperature and vertical velocity, can be described by circularly symmetrical Gaussian distributions at fixed distances from the fire (Hoult, Fay, and Forney 1969). Such distributions are used to describe the mean values of the temperature, effluent concentrations (of aerosols and molecular combustion products), and the vertical velocity of the plume when calculations are performed to predict the transmittance and turbulence effects. For a vertical plume, such a distribution has the form

$$A_d(r, z) = A_d(0, z) \cdot e^{-\frac{r^2}{2(\sigma(z))^2}} \tag{13}$$

where $A_d(...)$ is the parameter amplitude, r is the radial distance from the centerline, and $\sigma(z)$ is the diffusion function as a function of distance from the fire.

The distribution function behavior remains the same for the general curved plume used in FITTE, but the mathematical description becomes more complex. Conservation assumptions determine the decrease in peak amplitude of the parameters as a function of distance along the centerline. The general variation of the plume distribution functions is shown in figure 2.
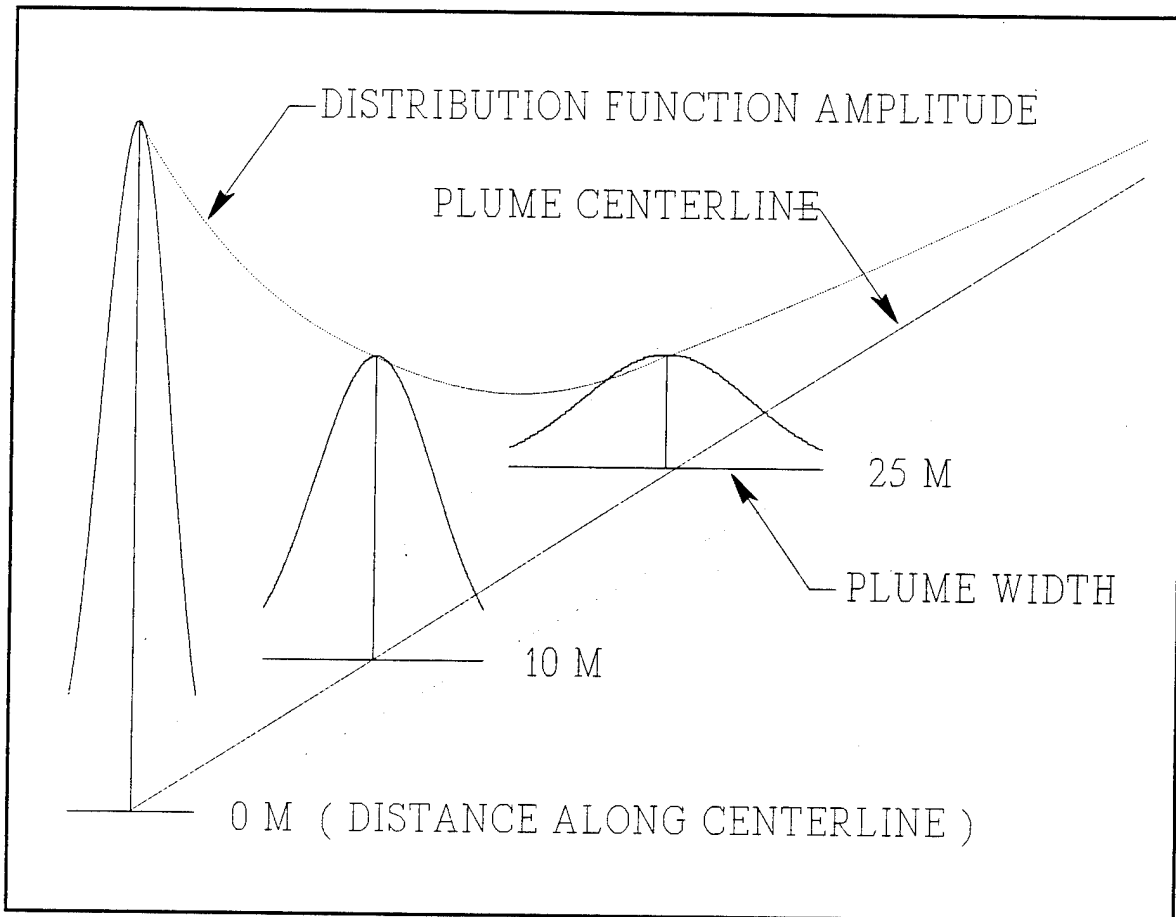
Figure 2. Plume distribution function behavior as a function of distance along the centerline from the fire.

18

The diffusion function σ is related to the entrainment parameter by

$$\sigma(D) = \sigma(0) + \frac{\xi D}{6.06} \tag{14}$$

and to the plume radius R by

$$R = 2.0\,\sigma(D). \tag{15}$$

The definition of the plume radius agrees roughly with the apparent plume edge seen by an observer. In performing the propagation integrals, FITTE uses the plume parameter distribution functions when a LOS point is within 3σ of the centerline (when the parameter is greater than approximately 1 percent of its peak value). The same radius is used for all the plume parameters.

The relation between equivalent top hat and Gaussian plume distributions has been described elsewhere (Thompson and DeVore 1981). For equivalent distributions, the integrated top hat values of mass, momentum, and buoyancy are required to equal truncated integrals of the corresponding Gaussian plume parameters. Figure 3 shows equivalent distributions, with the shaded portions in the left half indicating the areas mapped by the transformation between the distributions. The maximum of the Gaussian distribution is approximately 2.31 times the top hat amplitude for the effluent densities. The relation for the excess temperature above ambient is more complex, and the ratio ranges from about 2.3 to 2.9.
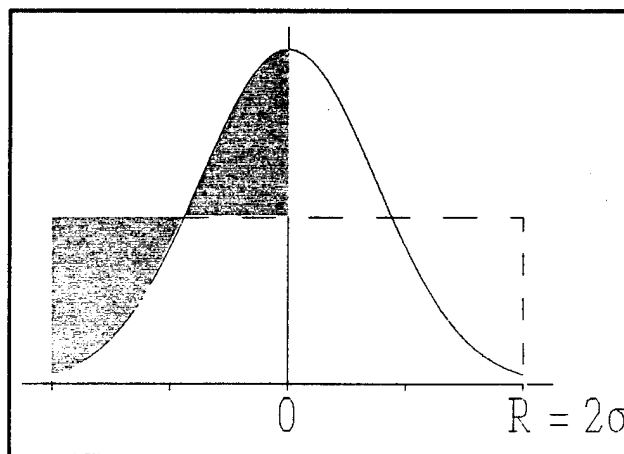
Figure 3. Equivalent top hat and Gaussian distributions.

The equation used to describe effluent aerosol concentration is based on the equation for a classic horizontal Gaussian plume;

$$\chi(x, y, z) = \frac{Q_M}{2\pi U\sigma^2} e^{-\frac{y^2}{2\sigma^2}} \left[e^{-\frac{(z - z_C)}{2\sigma^2}} + R_S e^{-\frac{(z + z_C)}{2\sigma^2}} \right] \quad (16)$$

where χ is the aerosol concentration at any point specified in the model coordinate system, Q_M is the aerosol mass emission rate, U is the mean ambient wind velocity, $\sigma(x)$ is the diffusion function, and z_C is the height of the plume centerline at x.

The effluent molecular combustion product concentrations are described in a similar fashion.

Equation (16) applies only in the extreme case of a horizontal plume. To include plume curvature or a vertical plume, the equation must be modified so the parameters are related to the direction of the mean flow at any point along the centerline. This transformation, although simple in principle, introduces geometrical and mathematical complexities, because the direction of the mean flow vector is a function of location for a curved plume.

For the general curved plume, the analog of equation (16) is

$$\chi(D, h, y) = \frac{2.31 Q_M}{4\pi S\sigma^2} e^{-\frac{y^2}{2\sigma^2}} \left[K_1 e^{-\frac{h^2}{2\sigma^2}} + K_2 e^{-\frac{(2h_C + K_3 h)^2}{2\sigma^2}} \right] \quad (17)$$

where D is the distance along the plume centerline to a point $(x_{CI}, 0, z_{CI})$, h is the distance (measured perpendicular to the mean flow vector S at D) from the plume centerline to the projection of a point $(x_L, 0, y_L)$ on the LOS onto the x-z plane, and h_C is the distance of the plume centerline from the ground (also measured perpendicular to S at D).

$\sigma(D)$ is related to the plume radius at D, as illustrated in figure 2. The coordinate y is the distance from the plume centerline perpendicular to the x-z plane.

20

The constants K_1, K_2, and K_3 in equation (17) take on values appropriate for specific situations. For a horizontal plume, $K_1 = K_2 = 1.0$. For a vertical plume, $K_1 = 1$ and $K_2 = 0$. The constants account for the reflection from the ground for quasihorizontal plumes. The conditions under which the model changes from one set of values to the other for bent-over plumes is described later. To obtain the appropriate value for the reflected concentration when there is reflection, K_3 is set equal to $+1$ if the point at which the function is to be evaluated lies above the centerline, or to -1 if the point lies below the centerline.

An accurate description of the plume temperature distribution is needed for calculations of the turbulence effects. If values from the equation for pressure equilibrium,

$$\bar{\rho}(r) \cdot \bar{T}(r) = \rho_A \cdot T_A = \rho_o \cdot T_o, \tag{18}$$

are substituted into the equation for the equivalence of mass,

$$\pi \bar{\rho} R_{TH}{}^2 = \int_0^{R_{TH}} 2\pi \rho(r)\, r dr, \tag{19}$$

the centerline temperature increment above ambient can be determined for an equivalent truncated Gaussian plume (one for which the integral of the top hat distribution is equal to the integral of the truncated Gaussian distribution). Overbars indicate the mean values associated with the top hat model. Experiments indicate that equivalence of the distributions should be defined for a top hat radius $R_{TH} = 2.0\ \sigma(D)$, which corresponds roughly to the visible edge of the plume. This definition leads to the expression for the centerline temperature:

$$T_C(z) = T_A \frac{\left[\, e^2 - 1\, \right]}{\left[\, e^{2T_A/\bar{T}} - 1\, \right]}. \tag{20}$$

21

The relations between the peak and mean values of the effluent concentration and the vertical velocity are found in a similar manner. It is assumed that all of these distributions are characterized by the same plume radius. Experiments (D. Bruce, unpublished data) indicate that this assumption is approximately correct.

Finally, the gradient of the amplitude of the plume temperature distribution must be found as a function of distance D along the centerline (or, alternatively, as functions of the centerline height z) for use in the turbulence effects calculations. This is done by expressing the centerline temperature as a function of z and taking the derivative with respect to z to obtain

$$\frac{dT_C}{dz} = \frac{dT_C}{d\bar{T}} \cdot \frac{d\bar{T}}{dz} \tag{21a}$$

where

$$\frac{dT_C}{d\bar{T}} = 2 \left[\frac{T_A}{\bar{T}} \right]^2 (e^2 - 1) \frac{e^{2T_A / \bar{T}}}{\left[e^{2T_A / \bar{T}} - 1 \right]^2} \tag{21b}$$

$$\frac{d\bar{T}}{dz} = T_A g F \left(\frac{2C^{3/2} R^2 z^{-1/2} + 6\xi U^{3/2} WR}{3U^{3/2} (F - gWR^2)^2} \right) . \tag{21c}$$

R and W are treated as explicit functions of z in arriving at equation (21c) and are treated as such in its evaluation.

The change in amplitude of the effluent flux distributions as functions of D are found by observing that the mass flow through all plume cross sections must remain constant to prevent buildup of mass at any location, so at any distance D from the origin, the effluent flux must be equal to the initial flux times the product of the plume velocity S and the cross-sectional area at the origin divided by the same product evaluated at distance D.

2.2.1.4 *Aerosol Optical Properties.*—Visual and IR aerosol optical parameters were based on theoretical calculations modified to give agreement with transmissometer data from BICT I. The aerosol-specific extinction coefficients

22

α for various wavelengths were based on Mie scattering theory calculations. The calculations used a theory (Chylek et al. 1981) that assumes carbon-based aerosols can be replaced by equivalent spheres with appropriate particle-to-void ratios. The theory was modified to give agreement with ratios of measured transmittance for different wavelengths. Details are given elsewhere (Sutherland and Walker 1982; Sutherland, Hoock, and Khana 1984) and will not be repeated here.

The values of single scattering albedo ϖ were derived from measurements of specific extinction and absorption (C. W. Bruce, private communication 1981) or were taken from Mie calculations (Khanna and Ammon 1983) for aerosol-size distributions and porosity characteristics based on measurements (Pinnick et al. 1982).

Table 2 lists the values used in FITTE. Interpolation is used to calculate the specific extinction coefficient and albedo at intermediate wavelengths. The 10.6-μm and millimeter wavelength values are from measurements (C. W. Bruce, private communication 1982).

Table 2. Particulate optical parameters

Wavelength (μm)	Specific Extinction Coefficient (m²/g)	Single Scattering Albedo
0.40	7.41	0.25150
0.55	5.57	0.25000
1.06	2.94	0.24493
1.50	2.23	0.24055
2.50	1.61	0.23060
3.80	1.34	0.21766
6.00	1.14	0.19577
8.50	1.01	0.17090
10.60	1.00	0.15000
8570.00	0.002	0.00000

2.2.1.5   *Fire Plume Fluctuations.*—The space-time variation of the fire plume is handled as a two-part model. The fluctuations of the plume about the mean centerline are treated as functions of windspeed and wind-direction fluctuations, while the fluctuations of the plume parameters are based on the assumption that they are dependent on turbulent mixing.

A time-history data file FIT4D.DAT is used to store the information needed for the fluctuation model in FITTE/FGLOW. The FIT4D.DAT file contains 2000 rows and 3 columns of data. The rows of data have a 1-s time increment and represent a time history of wind fluctuations since the start of the fire. Column 1 contains a random number (range: -0.5 to 0.5) used as input for calculating plume parameter fluctuations at a given time, column 2 contains the normalized cumulative fluctuation of the downwind (x-) component of the wind, and column 3 contains the normalized cumulative fluctuation of the crosswind (y-) component of the wind. The model was developed and tested with simulated data. Files developed from actual wind data as described in appendix A can be used after model operation is checked. The file structure is discussed further in appendix A, which gives information for creating a time-history file from wind data.

When FITTE is run, a current time is assigned. The current time may be the default time (100 s after the start of the fire) or another time read from an input file.

The displacement of any point P on the centerline from its mean position at the current time is calculated as follows: The distance along the mean centerline from the origin to point P is calculated using equation (12). The average plume velocity $\bar{S}$ to reach point P is half the sum of $S(P)$ and $S(0)$. The ratio of distance to mean velocity gives the time taken to reach point P from the fire. The time to reach point P from the fire is used to assign a source time (the time when the plume segment currently at point P left the source). The current time and source time are used as pointers to rows of the data array. Using the second (or third) column of the array, the difference in value between the values in these rows multiplied by the mean windspeed U gives the x- (or y-) displacement of point P from the mean centerline position. This permits calculation of the current position of point P to determine the plume parameter

distributions at points on an LOS near point P. Interpolation takes place when the time to reach point P is not an integer.

The random numbers in the first column of the FIT4D.DAT file are used in two ways:

(1) Assign scaled fractional fluctuations to the plume radius and to the heat and effluent production. The scaling limits the fluctuations to no more than 5 percent of the mean value of the corresponding parameter.

(2) The numbers are used as input for calculation of the fluctuations of the aerosol and effluent gas concentrations and of the plume temperature.

Modeling of the plume parameter fluctuations is based on the assumption that they are driven by atmospheric turbulence. Therefore, they should exhibit the same power spectral density distribution as found for atmospheric parameters within an appropriate frequency range. This is achieved by the choice of the coefficients used for the series that describes the fluctuations. The fluctuations are represented by a series with the following form:

$$\delta = \sum_{1}^{n} c_k \cos(b^k x + \varphi_k) \ . \tag{22}$$

The phase angles φ_k for the terms are obtained from the random numbers stored in the first column of the FIT4D.DAT file. Figure 4 is an example of a space- and time-varying (4D) plume.

2.2.2   The Radiative Transfer Model

The radiative transfer equation for a medium in which aerosol scattering and absorption and molecular absorption occur is

$$\frac{dI}{ds} = - \epsilon I + (\kappa_A + \kappa_M) B \tag{23}$$

25
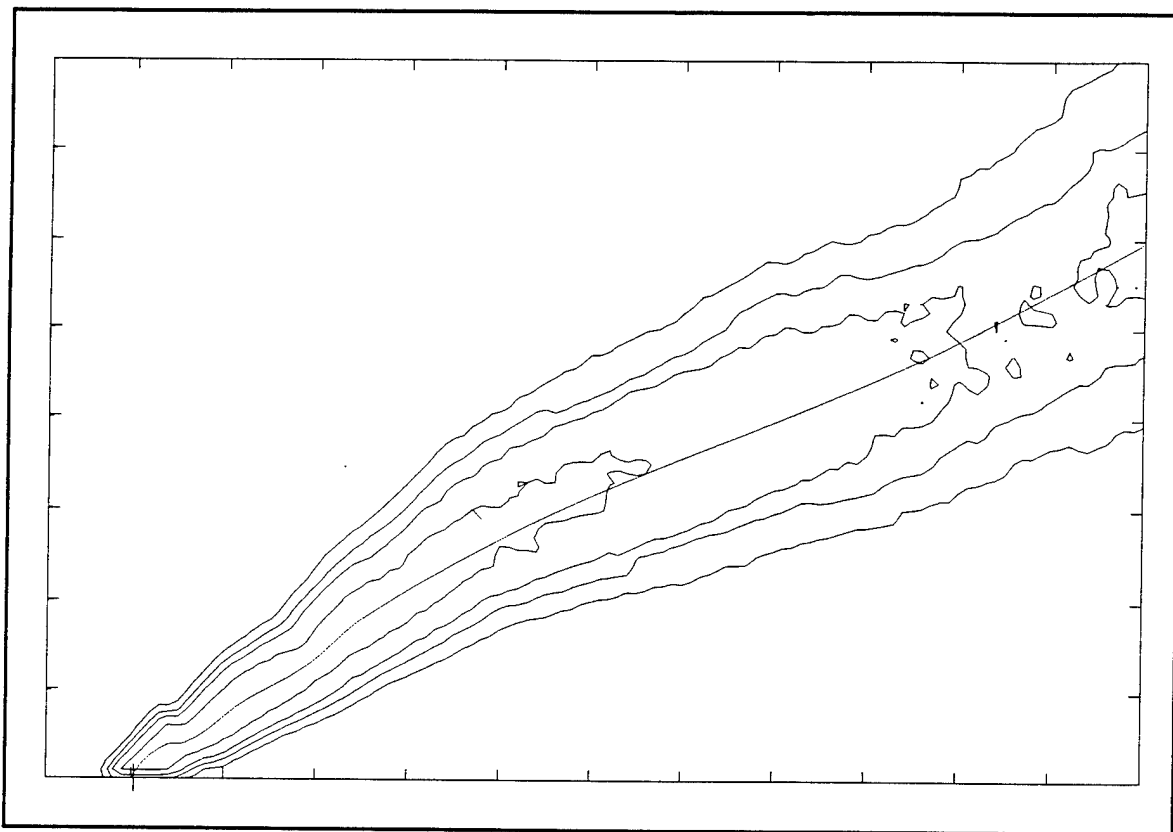
Figure 4. Contour plot of a space and time varying (4D) plume. Tic marks show 5-m spacing. The dashed line is the sketched centerline.

where I is the local spectral radiance (W/m^2/sr/cm), s is the distance along the LOS, ϵ is the total extinction coefficient (m^{-1}), κ_A and κ_M are the aerosol and molecular absorption coefficients (m^{-1}), and B is the blackbody function.

$$B(\lambda,\ T)\ =\ \frac{2\pi h c^2}{\lambda^5}\left[\ \frac{1}{e^{hc/\lambda kT}\ -\ 1}\ \right] \qquad (24)$$

where h is Planck's constant, k is Boltzmann's constant, and c is the speed of light in vacuum.

The radiance I has units of W/m^2/sr/μm, and the blackbody irradiance B has units of W/m^2/μm.

For the aerosol, the absorption coefficient κ_A is related to the extinction coefficient ϵ by

26

$$\kappa_A = (1 - \omega)\epsilon = (1 - \omega)\alpha\chi \qquad (25)$$

where α is the specific mass extinction coefficient of the aerosol (m²/g), ω is the single-scattering albedo, and χ is the local aerosol concentration (g/m³).

In FITTE, only the effluent aerosol and the major molecular combustion products (water vapor and carbon dioxide) are considered in the calculation. The aerosols are the dominant species for calculations in the visible and IR atmospheric window regions (Sutherland and Walker 1982; Khanna, Burlbaw, and Deepak 1982). If the path from target to observer is treated as a series of segments for which the effluent concentrations and temperature are nearly homogeneous, the radiative transfer equation can be integrated for each path segment to give

$$I = I_S e^{-\tau} + \frac{1}{\pi\epsilon}\left[(1 - \omega)\alpha\chi + \kappa_A B(1 - e^{-\tau}) \right] \qquad (26)$$

where τ is the optical depth of the segment, I is the spectral radiance in the segment, and I_S is the spectral radiance entering the segment from all previous segments.

The radiative transfer calculation is performed by evaluating this expression for each segment from the target to the observer using I for each segment and I_S for the following segment.

The extinction coefficients are functions of wavelength and temperature. The values used for the aerosol are temperature-average values from measurements; the values for the molecular combustion products are temperature dependent and are taken from the ATLES model (Young 1977) and unpublished data (Manning 1985).

The transmittance through the gaseous effluents of the fire plume and the molecular contribution to the emitted radiance are calculated by a band model adapted from the ATLES code (Manning 1985). For single wavelength calculations, the waveband is extremely narrow. The spectral resolution is not high but is dependent on the band model data base used and, generally, is

25 cm^{-1}. An important feature of the ATLES band model is its ability to treat temperature dependence if the data base contains parameters for high temperatures. This is the primary reason for choosing the ATLES model rather than the LOWTRAN code (Kneizys et al. 1983).

The band model was extracted from the ATLES code and adapted for use in FITTE. Code to perform calculations through aircraft and missile plumes was removed, large arrays were reduced in size by limiting the number of species the code can handle simultaneously and by limiting the size of the data base files that can be loaded, and the parts of the code that handle Doppler and Voigt line shapes were eliminated because only Lorentz line shapes are needed for FITTE.

The importance of temperature dependence was described (Manning 1985). Manning points out that, at high temperatures, transmittance is not strongly affected in the 2500-cm^{-1} region, but it is greatly reduced in the 2000- and 3300-cm^{-1} regions as hot-band transitions from nearby carbon dioxide and water vapor bands become active. Because the radiance emitted in a spectral band increases as transmittance decreases, correct prediction of transmittance in the fire plume is important.

The band model parameters included for use in FITTE are taken from four files: two for carbon dioxide and two for water vapor. The files were combined into a single file called BPARAM.DAT. The carbon dioxide section of the file covers the spectral region 2000 to 2400 cm^{-1}, which includes the important carbon dioxide fundamental band at 4.3 μm (2300 cm^{-1}) and the region from 3100 to 3700 cm^{-1}. It includes temperature data at 10 temperatures from 100 to 3000 K. The water vapor section of the file covers the spectral regions from 50 to 2500 cm^{-1} and from 2500 to 4500 cm^{-1}. It contains data at seven temperatures between 300 and 3000 K. The BPARAM.DAT file represents most of the important absorption bands of carbon dioxide and water vapor in the IR. The carbon dioxide files were supplied with the ATLES code. The water vapor files are later, unpublished data (Manning 1985).

When the input file specifies that calculations are to be performed for a spectral band, propagation is calculated using ATLESF for a number of wave numbers across the band. The values are used to predict values for a selected sensor

response function for the waveband. The radiance is integrated over the band, and the transmittance is averaged over the band. Calculations are made using equations (27) and (28).

If $I(v)$ represents spectral radiance ($W/m^2/sr/cm$), and $f(v)$ represents an instrument spectral response function with a range of zero to one, the integrated radiance is given by

$$I = \int I(v)\, f(v)\, dv \qquad (27)$$

and has units of $W/m^2/sr$.

The average transmittance over the band is

$$\Theta = \frac{\int \Theta(v)\, f(v)\, dv}{\int f(v)\, dv}. \qquad (28)$$

Note the difference in the two calculations. The radiance is an integrated quantity; if the radiance is constant with wave number and the instrument response function is a rectangular function, increasing the size of the rectangular window should increase the radiance. The transmittance is an average over the band; if the transmittance is constant with wave number and the size of the rectangular window is increased, the average transmittance should not change.

2.2.3 *Fire Plume Turbulence Effects on Laser Beam Propagation*

Prediction of the effects of fire plume turbulence on propagation requires the use of a stochastic model. The turbulent hot plume can be regarded as a variable density lens that changes with time. The driving forces for the fluctuations are entrainment and turbulent mixing of ambient temperature air into the plume. It is assumed that existing theory for laser beam propagation through the turbulent atmosphere can be used if appropriate changes are made to the definitions of parameters and the ranges in which they are valid. The key assumption is that the index of refraction structure constant C_n^2 must be replaced by a structure function within the plume dependent on the

time-averaged temperature distribution. The gradient of the time-averaged temperature distribution determines the step size that must be used to obtain accurate results from the calculations.

The turbulence effects model predicts values of laser beam parameters at the target that depend on the turbulence-induced fluctuations in the LOS index of refraction. It is a modification of a model developed (Thompson and DeVore 1981) for ASL based on work in the literature (Fante 1975). The magnitudes of the propagation effects are a complex function of the wavelength and of the relative sizes of the laser beam and the plume.

The index of refraction structure constant (Tatarski 1971) is given by

$$C_n^2 = \frac{\left\langle \left[\tilde{n}(r_2) - \tilde{n}(r_1) \right] \right\rangle^2}{\left(r_{12} \right)^{2/3}} \tag{29}$$

where $\tilde{n}(r_i)$ is the instantaneous fluctuation in index of refraction at point r_i and r_{12} is the distance between points r_1 and r_2.

The brackets denote an ensemble average over all points (in a localized region) separated by the distance r_{12}. In practice, an ergodic hypothesis is invoked to replace the ensemble average by a time average.

The index of refraction of air is given by (Strohbehn 1978)

$$n = 1.0 + 77.6 \times 10^{-6} \frac{P}{T} \left[1.0 + \frac{7.52 \times 10^{-3}}{\lambda^2} \right] \tag{30}$$

where P is the pressure (mbar), T is temperature (K), and λ is the wavelength of interest (μm).

A humidity-dependent term negligible at visual and IR wavelengths was omitted. Examination of equation (30) shows that temperature fluctuations cause index of refraction fluctuations.

For atmospheric turbulence in which the temperature fluctuations are of the order of 1 K, the variance of the index of refraction is proportional to the

variance of the temperature. For turbulence in fire plumes in which temperature fluctuations are of the order of tens or hundreds of degrees, the variance of the index of refraction must be related to that of the reciprocal of the temperature:

$$\sigma_n^2 = A_n^2 \left(\sigma_{1/T} \right)^2 \tag{31}$$

where

$$A_n = (n - 1)T. \tag{32}$$

The index of refraction structure constant is obtained from the relation

$$C_n^2 = 1.91 \left(\frac{\sigma_n^2}{L_o^{2/3}} \right) \tag{33}$$

where L_o is the outer scale of turbulence (Tatarski 1971).

Effects of turbulence on propagation in the atmosphere are calculated using the assumption of Kolmogorov spectral distribution of index of refraction fluctuations. L_o is the outer scale of turbulence (the size of the largest eddies for which the energy cascade to smaller eddies is linear), and l_o is the inner scale. For the atmosphere, L_o is of the order of tens of meters and l_o is of the order of millimeters. L_o is actually an inverse function of height above the ground for neutral and unstable Pasquill stability categories and is approximately constant for a stable atmosphere (Wyngaard 1973).

For turbulence in fire plumes, the Kolmogorov spectral distribution is used with the outer scale L_o set equal to the radius of the plume. Values of C_n^2 inside the warm region of the plume are typically one to three orders of magnitude higher than ambient values. To evaluate C_n^2 along the path, it is necessary to assume a temperature probability distribution about the mean temperature at any given point. The time-averaged temperature distribution in the plume, in a plane perpendicular to the centerline, is a circularly symmetrical Gaussian distribution with the following form:

$$T = \left(T_C - T_A \right) e^{-\frac{r^2}{2(\sigma(D))^2}} + T_A \tag{34}$$

31

where T is the time-averaged temperature at point p, T_C is the centerline temperature, T_A is the ambient temperature, r is the distance of point p from the centerline, and $\sigma(D)$ is the diffusion function that specifies the local plume width.

The centerline temperature is obtained from the plume model, and the average temperature at point p is used to predict the value of $C_n^2(p)$ in the turbulence effects calculation. In actual calculations, the simplified exponential expression of equation (33) is replaced by the exponential terms of equation (17).

FITTE uses established turbulence theory (Fante 1975) to find the diffraction limited spot radius (ρ_D), lateral coherence length (ρ_o), short- (ρ_s) and long-time (ρ_L) average spot radii, and average instantaneous distance of the centroid (ρ_c) from its long-time average position. The parameters are used to predict a centroid jitter radius and a spot area magnification ψ.

The increase in the instantaneous beam area at the target is calculated from

$$\psi = \left(\frac{\rho_s}{\rho_D} \right)^2 \tag{35}$$

where ρ_D is the diffraction limited spot radius at the target.

This result can be used to estimate the average decrease in intensity at the target. No detailed information about spot intensity distributions is predicted because the distributions are a function of relative beam and plume sizes, the variations in path integrated particulate concentration for incremental areas of the spot and the fluctuating lens represented by the plume.

For the points outside the plume, the simplifying assumption made is that C_n^2 is constant and equal to 1.0×10^{-14} m$^{-2/3}$. The model is not sensitive to the value chosen.

For plume temperatures less than 10 °C above ambient, an approximation is used to evaluate the variance of the index of refraction. For equation (36) (George, Alpert, and Tamanini 1977)

32

$$\sigma_T^2 \approx 0.4 \left(\overline{T} - T_A \right) \tag{36}$$

where $\overline{T}$ is the mean temperature at a point,

and the approximate relation

$$\sigma_n^2 \approx A_n^2 \frac{\sigma_T^2}{\overline{T}^{-4}} \tag{37}$$

can be used in equation (33) to find C_n^2. The values obtained for σ_n^2 using this approximation give satisfactory results in the prediction of centroid jitter when compared with experiments (D. Bruce, unpublished data).

When the turbulence is not yet fully developed within a distance from the fire of four times the source radius, a separate method is used to calculate C_n^2. The method, described elsewhere (Thompson and Devore 1981), relates the variance of the temperature structure function σ_T^2 to the mean temperature gradients in the plume and assumes partial mixing of ambient air in this region. C_n^2 is calculated from equation (33), but equations (36) and (37) are replaced by

$$\sigma_T^2(D, r) = 3L_o^2 \frac{(\nabla T(D, r))^2}{1.91} \tag{38}$$

and

$$\sigma_n^2 = A_n^2 \left[\frac{\sigma_T^2}{(T_A T_M)^2} \right] \tag{39}$$

where T_M is the temperature of the partially mixed fractional volume of air.

This method of calculation is invoked automatically by the model when the LOS passes through the incompletely mixed region of the plume.

2.3   Model Implementation

2.3.1   FITTE

FITTE performs calculations to predict effects for specific LOS. FITTE/FGLOW has three defined scenarios. Scenarios 1 and 2 are single LOS (FITTE) scenarios used to predict the effects of the fire plume on general systems such as laser designators, and laser- or other seeker systems. Scenario 3, discussed below as FGLOW, performs calculations for multiple LOSs to predict radiant images of fires that may affect imaging systems such as IR cameras.

Scenarios 1 and 2 have identical geometry, as seen in figure 5, but differ in the direction of the turbulence calculation. Separate calculations are needed because calculation results depend on path-weighted averages. The target and emitted radiance are calculated as seen from the observer position for both scenarios. For scenario 1, the turbulence effects are calculated at the target position; for a laser beam propagating from observer to target. For scenario 2, they are calculated at the observer position; for a reflected laser beam propagating from target to observer.

2.3.1.1   *Scenario 1.*—Scenario 1 corresponds most nearly to the original version of FITTE, and it is the default for running the model. The observer can be any of the following: a laser designator, an observer with night-vision goggles, or a visible or IR imaging system. The target has no assigned physical dimensions but may have a nonambient temperature and emissivity. The radiative transfer calculations are performed so the values produced are given at the observer position. The transmittance applies at either end of the path. Unless a waveband calculation is specified, turbulence effects parameters for the beam (assumed to be a laser beam) are predicted at the target position.

Various combinations of output parameters can be used to predict quantities such as the relative laser intensity on the target (initial intensity times transmittance divided by spot magnification), target contrast (target radiance divided by the sum of target and emitted radiances), etc.
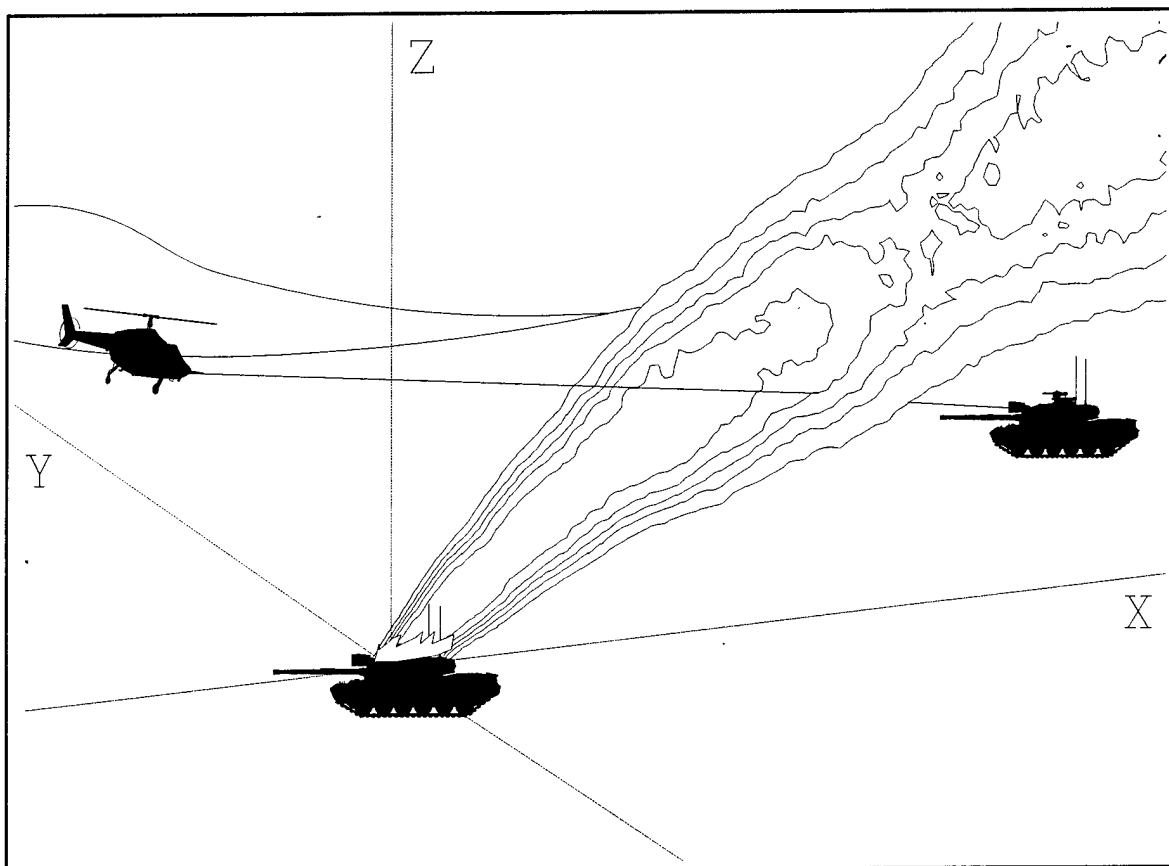
Figure 5. Geometry for the single LOS scenarios. The helicopter carries a laser designator for scenario 1 or a laser-guided munition for scenario 2.

2.3.1.2   *Scenario 2.*—Scenario 2 is used much the same way as scenario 1 and performs the same calculations for radiative transfer. It was included for the calculation of turbulence effects on a laser beam reflected from the target to the observer. The effects are different from the effects in scenario 1 for all cases in which the fire plume is not at the center of the propagation path, because the turbulence in the plume distorts the wave front in a manner similar to a set of diverging lenses; therefore, the net effects depend on the path-weighted plume turbulence.

Time-series calculations can be performed for these scenarios to give tabular output of the parameters. Figure 6 shows graphs of the predicted fluctuations of several parameters.
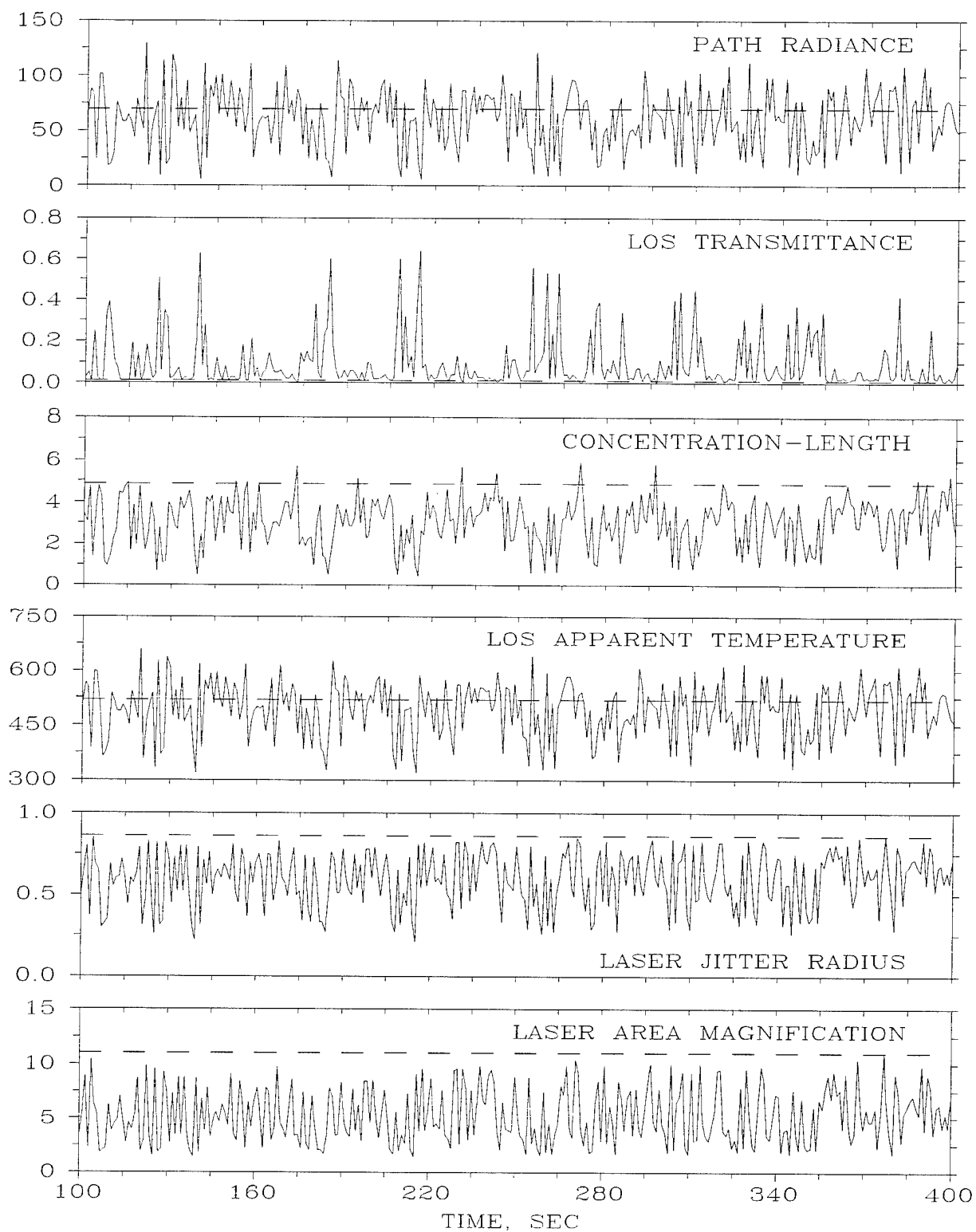
Figure 6. Graphs of model output data for a time-series calculation at 10.6 μm. The dashed lines show the values predicted by the mean-value model.

2.3.1.3 Geometric Relations for Plume Parameters on the LOS.

—Because integration along the LOS is required to evaluate the fire or plume effects, geometrical relations are needed to predict plume parameter values at points on the LOS. The plume parameters are expressed as functions of the distance along the centerline and of the radial distance from the centerline to the point on the LOS.

Any point p on the LOS has a projection $(x_L, 0, z_L)$ on the plane of the time-averaged plume centerline, and the shortest distance from the centerline to the projected point is along a line perpendicular to the centerline. The equation of any such line has the form

$$z = mx + b \qquad (40)$$

where m is the negative inverse of the centerline slope at a point $(x_{CI}, 0, z_{CI})$;

$$m = \left[-\frac{1}{dz/dx} \right] = -\frac{3}{2} \left(\frac{U}{C} \right)^{3/2} \sqrt{z_{CI} + z_V} \ . \qquad (41)$$

Because $(x_L, 0, z_L)$ is also on the line, the intercept b is given by

$$b = z_L + \frac{3}{2} \left(\frac{U}{C} \right)^{3/2} \sqrt{z_{CI} + z_V} \ x_L \ . \qquad (42)$$

An equation for z_{CI}, the centerline point closest to $(x_L, 0, z_L)$, is found by substituting equations (41) and (42) into equation (40) and replacing x_{CI} by substitution from the centerline equation. The equation obtained is

$$\frac{3}{2} \left(\frac{U}{C} \right)^3 (z_{CI} + z_V)^2 + (z_{CI} + z_V) - \frac{3}{2} (x_V + x_L) \left(\frac{U}{C} \right)^{3/2} \sqrt{z_{CI} + z_V} - z_V - z_L = 0. \qquad (43)$$

Equation (43) can be solved by the substitution

$$Z = \sqrt{z_{CI} + z_V} \qquad (44)$$

and subsequent use of the solution for quartic equations found in the CRC© Standard Mathematical Tables (Beyer 1981).

The distance of any point on the LOS from the closest centerline point can be found and used to evaluate the plume parameters.

The distance from the centerline point to the projection of the LOS point on the x-z (wind-aligned) plane is denoted by h. The distance from the plume centerline to the ground along the same line is defined as h_g. When h_g is greater than 2.0 σ, the constants K_1 and K_2 in the plume equations are set to the values for a vertical plume because no reflection from the ground occurs.

2.3.1.4   *Information about Calculations along the LOS.*—For radiance and transmittance calculations, the default number of calculation intervals through the plume is 30, giving a step length of 0.2 σ. This does not affect the model accuracy for most LOS. Step size effects are most likely to occur for LOS near the plume centerline and very close to the fire. The calculation of turbulence effects is performed using an adaptive Simpson's rule integration subroutine, ASRI, rather than a fixed number of calculation intervals. A single calculation interval is used between the plume and the observer when molecular absorption calculations are performed.

When waveband calculations are performed, the molecular effects subroutines (the ATLESF set) are called for the first interval, and subsequent calls are made only when the temperature change from the previous interval exceeds a fraction (default = 0.1) of the previous value.

2.3.2   *FGLOW: Fire/Plume Radiant Emission and Transmittance*

FGLOW is an extension of FITTE that performs calculations for multiple LOSs to generate a simulated image matrix. It does not calculate turbulence effects on laser propagation.

Figure 7 shows scenario 3, the FGLOW scenario. An imaging system is located at the observer position with its LOS specified by a target position, and a fire or a plume segment is within the field of view. FITTE calculates the emitted radiance for an array of pseudotarget positions to create a file that contains a matrix representation of the radiant image of the fire and

38

transmittance of the plume. The array is defined by an input card to have n rows, m columns, and an angular resolution (in milliradians) between elements.
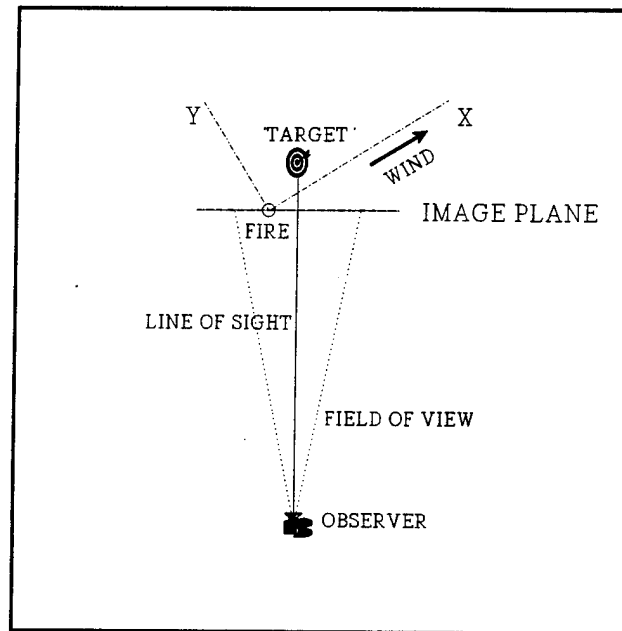
Figure 7. Top view of scenario 3 (FGLOW) geometry. Situation shown is for the 240° wind direction of example 9.

Because the calculation matrix for FGLOW typically contains many LOSs that do not pass through the plume, the model sets a flag and stores the values calculated for the first LOS that does not intercept the plume. Calculation speed is increased by using these stored values for all subsequent LOS that do not intercept the plume.

3. Caveats

3.1 Grade of Software

The FITTE model should be classified as a research model. This choice of software grade is based on the fact that no quantitative evaluations were made for the spatial and time variations introduced into the model and for the limited evaluations of predictions of beam wander and spread.

3.2 Model Failure

The model fails to run if selected input values do not meet acceptance criteria. Failure occurs if: (1) the observer and target positions are on the same side of the wind-aligned axis in the model coordinate system, or (2) either waveband limit on the BAND card is outside the range of the molecular absorption data in BPARAM.DAT.

The model fails to run if: (1) the files BPARAM.DAT and FIT4D.DAT are not located in the same directory as the executable program, (2) a non-EOSAEL format input card is encountered, or (3) an unexpected end-of-file is encountered in an input file.

The model fails if the disk runs out of space for the output files. The model is most likely to fail if FGLOW is run for a large image matrix or a time-series of smaller FGLOW images.

Caution must be exercised under the following conditions:

• The model runs if many of the possible input parameters are out of bounds. In this case, a default value is substituted for the out-of-bound parameter, the output file contains a message stating DEFAULT(S) REPLACE INVALID INPUT ON CARD *CARDNAME*, and the default values appear in the printout of input parameters contained in the output file.

• Bounding values are set for a parameter if the value is known to be physically bounded (target emissivity must be between 0 and 1) or if an out-of-bound value affects the accuracy of model computations (windspeed must be greater than 0.10 because it appears in the denominator of several equations).

41

• The model performance was tested only under relatively benign atmospheric conditions: windspeeds less than about 10 m/s (22 mph) on clear or cloudy days with unstable or neutral stability. Model performance is expected to degrade under more severe weather conditions, but it is not known how rapid or severe the degradation will be. No provision exists for including effects of obscurants such as rain, fog, or smoke clouds with the effects of the fire plume.

3.3   Verification Tests

Model verification was obtained from laboratory and field tests. All comparisons to date were made with the predictions of the Gaussian plume model. This is the most meaningful approach to the question of general model validity because time-averaged data correspond well with a Gaussian plume (D. Bruce, unpublished measurements). Transmittance, radiance, and plume centerline shape and spread for the time-averaged plume agree well with field test data. The laser wander and beam spread predictions were verified by laboratory experiments. Aerosol-specific extinction, generally, agrees well with laboratory and field data, but visible and near-IR values of albedo are low compared to measured values.

Comparisons with field data suffer from various problems. If point measurements are made, the results depend strongly on plume meander because of changing wind conditions. If the instruments are at fixed positions, it is possible to obtain little or no data. If data are obtained, auxiliary measurements are needed to determine the location of the probe within the plume relative to the instruments. If, as at the BICT III test, a crane is used to position an instrument cage within the plume, data are obtained, but the data reduction problem of relative position is even more difficult. Similar problems occur for transmittance measurements that represent LOS integrated data. As a result, limited data are available because of difficulties encountered in making measurements through plumes in the field and in analyses of the data.

3.3.1   Fire and Plume Properties

The shape of the time-averaged plume centerline (Briggs 1969) was based on extensive observations of plumes from smokestacks under a variety of meteorological conditions. The applicability of this model to ground-level

small fires was verified by comparing visible plume images (photographs or video) with model predictions for appropriate fire size and wind conditions. Good agreement was reported (Bruce and Sutherland 1986).

The plume centerline angle of elevation depends on the ratio of the vertical velocity to the (horizontal) windspeed. Plume angles of elevation as a function of windspeed were reported (Hall and Manning 1986) from imagery taken at BICT III. Digitized images from each of 10 data segments were used in the analyses. The data segments were chosen to represent a range of windspeeds. After reclassifying the windspeed for two segments of the data, the authors found a linear relation between angle of elevation and windspeed for windspeeds ranging from 1 to 7 m/s. The authors mention that uncertainties are introduced in determining the position of the origin of the plume and the need to ignore centerline curvature (Hall and Manning 1986).

Figure 8 shows the measured values compared with model predictions for the fire type (2) closest to the BICT III fires. The error bars indicate the standard deviation of the data. Agreement is reasonable, but the difference in slope indicates that changes in the model would be appropriate. The changes should probably involve an increase in thermal flux as a function of windspeed. Experiments are currently being conducted to determine effects of windspeed on fire and plume parameters.

Another important measure for the plume model is how well it predicts plume spread. The ability of the model to predict plume spread can be verified by comparisons of total angular spread observed in images with the value obtained from the entrainment parameter ξ for various windspeeds. This type of comparison was made for a number of plume images, and, with the assumption that the visible plume edge is at the 2σ point of the model Gaussian distribution, agreement is good. This means that the model predictions are typically within the range of uncertainty for the measured values.
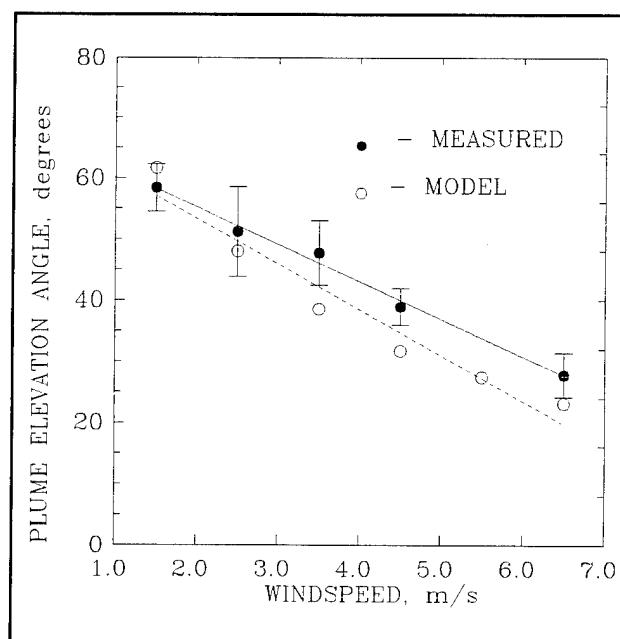
Figure 8. Comparison of measured and modeled plume elevation angles.

3.3.2 Aerosol Optical Properties

Laboratory and field measurements of aerosol optical properties in plumes from diesel fuel fires were reported. Figure 9 shows a comparison of extinction coefficients from FITTE with laboratory data (Bruce et al. 1991). The measurements were made with a flowthrough photoacoustical system with an incorporated short-path transmissometer from which data is obtained for both specific absorption and extinction coefficients. Correlated measurements of aerosol characteristics were obtained by timed collection of filter samples and subsequent analyses to obtain total particle weight, particle size distribution, and chemical identification. Error bars indicate variations of measured values with the naturally occurring variation of aerosol size distribution during a series of experiments. Agreement at 10.6 μm is due to the fact that the measured values at that wavelength were used to determine the absolute scale for the Mie calculations used for the model optical parameters at other wavelengths.

44
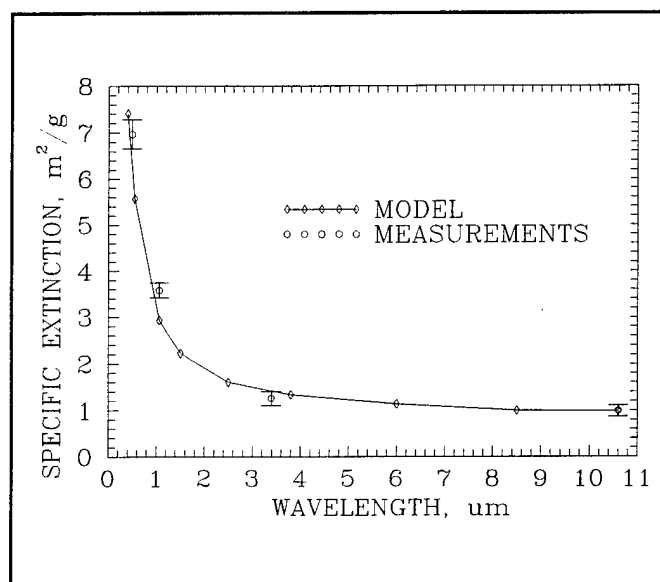
Figure 9. Comparison of measured and modeled extinction coefficients.

Two series of field measurements (Bruce and Richardson 1983; Bruce et al. 1989) of optical properties of diesel fire plume aerosols at 10.6 μm gave extinction coefficients averaging about 20 percent higher than those for the laboratory measurements and showing a greater variability than the laboratory data. We attribute the increased values to the presence of a greater number of large aerosols in the measured size distributions. The values from the field data (1.3 ± 0.7 and 1.2 ± 0.3 m²/g) overlap the laboratory value (0.99 ± 0.12 m²/g).

The modeled and measured values of single scattering albedo are compared in table 3. The measured values are from the same laboratory experiments as the specific extinction and are calculated using the formula $\omega = 1 - \alpha/\varepsilon$. No value was obtained at 1.06 μm because no gas that absorbs strongly at this wavelength is available to provide calibration data for the spectrophone, and changes in beam geometry for different wavelengths preclude the use of calibration from other wavelengths (C. W. Bruce, private communication).

45

Table 3. Comparison of albedo values

λ (μm)	ϖ_{MODEL}	$\varpi_{MEASURED}$
0.488	0.25062	0.34720
3.390	0.22174	0.32540
10.600	0.15000	0.15000

The substantial difference between the modeled and measured values at shorter wavelengths indicates problems with the values currently used in the model. Revision of the values await data at additional wavelengths, since the functional dependence is highly non-linear in the short wavelength region. The use of Mie calculations, valid only for spherical particles, and particle-to-void theory for the stringy aerosol particles is subject to large uncertainties, as was the assumption that the particles could be described by a bimodal size distribution. The primary effect on model output is a change in predicted emitted radiance at visual and near-IR wavelengths. Experimental runs using measured values, and with scaled increases in albedo values at intermediate wavelengths, indicate that emitted radiance decreases by 12 to 15 percent in the visual and near-IR wavelength regions.

3.3.3 Plume Distribution Functions

Radiant emission, measured with thermal imaging systems during the Battlefield Emissive Sources Trial, Oldebruck, the Netherlands, Europe (BEST ONE) test, was used to check the predictions of FGLOW. Images were analyzed to give the time dependence of the total area that exceeded various blackbody equivalent temperatures (S. B. Crow, private communication). Good agreement of measured and simulated radiation temperature spatial distributions was obtained for top hat source temperatures ranging from 1223 to 1473 K (Bruce 1989). This is roughly 300 K higher than the value currently used for the model. Peak temperatures measured close to the edge of one of the fuel drums during the BICT III test were approximately 1250 K (D. Bruce, unpublished data). Calibrated imagery taken at BEST ONE with short- and long-wavelength cameras and several narrow-band filters (Leidner and Clement 1987) show maximum radiation temperatures between 800 and 1300 °C for an open tray fire and between 600 and 900 °C for burning vehicles of which the flames were mostly enclosed.

46

Peak vertical plume velocities measured at the BICT III test (Bruce et al. 1989) were approximately 2.9 m/s at 3 m from the fire and 1.2 m/s at approximately 14 m from the fire.

Molecular combustion product concentrations in diesel fire plumes were measured (Bruce et al. 1989; Kaaijk 1986). Maximum measured carbon dioxide concentrations ranged from 100 ppm to >1000 ppm above the ambient concentration, and the maximum measured water vapor increase ranged from 0 to 7 mb above ambient. Other effluent gases occur in very low concentrations. Benzene was the prevalent aromatic hydrocarbon, with a measured concentration range of 0.3 to 3.0 mg/m^3 (Kaaijk 1986), and carbon monoxide concentration was less than 100 ppm because it was not detected by the chemical analyses. The concentrations reported by Kaaijk represent an average value for the plume position during the sampling time, while those reported by Bruce et al. include instantaneous as well as time-averaged values. The concentrations in both cases were measured approximately 15 m from the fire. The measurements can only be used to determine if the effluent concentrations used in FITTE are approximately correct.

The carbon dioxide concentration was chosen for comparison with the model because it is a more direct measurement. The assumption was made that the mean concentration at a distance of 15 m from the base of the plume was approximately 667 ppm. Data given for plume spread and fire size (Bruce et al. 1989) were used to estimate values at the source and obtain a mean concentration of approximately 8000 ppm; much less than the 136,000 ppm modeled in earlier versions of FITTE. The very large number was obtained based on the assumption (Manning 1985) that the effluent gases represented 100 percent of the gases above the fire and the fact that the effluent gas concentrations were not modeled as dependent on the burn rate. The current model for effluent gas concentrations ties their values to the rate of fuel consumption and results in source concentrations of carbon dioxide between 6000 and 17,000 ppm, in satisfactory agreement with the measured values.

The aerosol mass concentrations reported from filter data (Kaaijk 1986) ranged from 0.001 to 0.036 g/m^3 and were not corrected for the time the sampler was not in the plume or for the fact that the sampling system was usually near the edge of the plume when it was within the plume. The time in the plume varied

47

from less than 10 to 70 percent of the 20-min sampling period. The peak aerosol mass concentrations derived from optical measurements within the plume (Bruce et al. 1989) were typically 0.500 g/m^3, with an observed maximum value greater than 0.640 g/m^3. The same estimation procedure used for the source gaseous effluent concentration gives a source aerosol mean mass concentration of approximately 2.6 g/m^3; approximately 20 percent higher than the value used in the model.

A less direct indicator of the adequacy of the plume distribution functions is given by comparison of measured and simulated transmittance. The comparison depends on accurate optical parameters as well as the distribution functions and must be performed with appropriate matching of beam parameters. Comparisons of measured transmittance at BEST ONE with FITTE predictions were reported (Gillespie 1987; Bruce 1989). The results for this test are compromised by the fact that no survey data are available to provide reliable position data.

Gillespie used a modified version of FITTE (Manning 1985) available in early 1987 with calculations from the PC version of LOWTRAN to account for transmittance effects of natural aerosols. This version of the model did not perform area averaging for large beam sizes. Trials were divided into two classes according to the magnitude of transmittance change during the trial. Results of comparing simulated single wavelength visible with measured broadband visible data were poor, typically differing by more than 20 percent. Results at 1.06 μm were generally better, differing within 10 percent for five trials and greater than 20 percent for four. In the 3- to 5-μm band, differences were less than 10 percent for five trials, less than 20 percent for three trials, and greater than 20 percent for two trials. In the 8- to 14-μm band, differences were less than 10 percent for two trials, less than 20 percent for three trials, and greater than 20 percent for four trials. Gillespie categorizes the results as a fair validation of FITTE.

A number of factors probably account for some of the disagreement. The measured transmittance at 1.06 μm is lower than in the visible band for most of the tests used in the comparison. A later test (Farmer et al. 1989) suggests that the results could be caused by vignetting of the beam at one of the wavelengths, operation of a detector in a nonlinear response range, or

48

misalignment of the optical system. For all wavelengths, there were a number of trials for which no comparison was made because the model indicated that the LOS did not pass through the plume. This indicates problems with the available input data and may have affected all aspects of the comparison.

Bruce used the revised version of the 1987 FITTE module to perform comparisons for one of the BEST ONE trials. She varied the fire parameters to obtain good agreement with calibrated IR imagery, and used the area averaging feature of FGLOW (the angular resolution was chosen to match the transmissometer beam size) to find transmittance at three IR wavelengths for a variety of positions in the plume. The area near the estimated position of the transmissometer LOS was examined, and an area was found in which agreement of simulation and measurements was less than 25 percent for all wavelengths.

3.3.4   Effects of Thermal Plume Turbulence on Laser Beam Propagation

Concurrent laboratory measurements were made of temperature fluctuations in plumes and of laser beam spread and jitter for a beam traversing the plume (Bruce and Sutherland 1986). The experiments verified the method used to calculate the localized turbulence structure function within the plume. The measured plume centerline temperature and radius were used to tailor the FITTE plume for simulations that showed that the FITTE predictions of laser beam wander are good (within 10 percent) and predictions of beam spread are good to satisfactory (within 15 to 25 percent) for regions outside the flames. The errors are greatest in the region just outside the flames. The experimental data identified a method of calculation to be used for the area close to the fire in which the plume is not yet well mixed.

4. Operations Guide

FITTE can be run using the standard EOSAEL driver. It is also furnished with a dedicated driver for use on a PC. If the driver is used, link the FITTE subroutines with the program FITDRV.FOR, found in the FITACC directory. FITDRV.FOR contains several subroutines and a block data file EOSLBD. Several example auxiliary programs are furnished that can be used to create pseudogreyscale printouts of FGLOW output or to modify the FGLOW output files for use by programs that can create contour plots. These examples are described in appendix B.

The discussion and examples in the manual apply to the code and information supplied by the author to the custodians of the EOSAEL library. Some of them may not apply to the actual distribution. Check the distribution for documentation files that may give information on changes in the code. The example files furnished with the distribution were produced with that version of the code.

4.1 Input

The input cards (actually input file records) use the standard EOSAEL format (A4, 6X, 7E10.4). Run repeated scenarios with the usual EOSAEL procedure. Six to nine data cards, normally, are used with GO and DONE cards controlling program execution. Tables 4 through 17 contain descriptions of the FITTE input cards. The accompanying text gives additional information about some of the cards, including definitions of new cards and changes to some previously defined cards.

Running the model with the standard EOSAEL driver requires an EOSAEL WAVL card and a card to call the FITTE module. Usually, it also requires the cards REFD, SCEN, SRCL, METD, and DETD or SCN3. SCEN and METD may be omitted if the data were furnished to EOSAEL main, in which case, flags, used as FITTE calling parameters, indicate the need to convert the data units. Use all other cards to invoke various model options.

REFD contains information about the orientation of the user coordinate system and several model control parameters. The position data for the observer and target, given on the SCEN card, and for the fire, given on the SRCL card, can be in any convenient right-handed coordinate system. Give the *x*-axis heading of that (user) coordinate system. The heading and the wind direction on the METD card are given by angles measured clockwise from north. Use the control parameters on REFD as indicated.

Table 4. The REFD card

Identifier REFD	Variable	Default	Description Reference data
	XHEAD		*x*-axis heading of user coordinate system (degrees clockwise from north)
	ITYPE	1	code for fire type (1 through 4) 1 - jeep 2 - truck 3 - tank 4 - small fuel depot
	ISCN	1	code to specify FITTE scenario (1 through 3) 1 - propagation from observer to target 2 - propagation from target to observer 3 - predict propagation to imager
	IAVG	0	code to choose time-averaged plume calculation: 0 or positive number $\Rightarrow$ use 4D plume negative number $\Rightarrow$ use time-averaged plume
	NTURB	0	negative value cancels turbulence calculations

The SRCL card contains the position of the origin of the FITTE coordinate system in the user coordinate system. The x-axis of the FITTE coordinate system is aligned with the wind vector.

Table 5. The SRCL card

Identifier SRCL	Variable	Default	Description Fire location data
	US(1)		x-coordinate of center of fire (m)
	US(2)		y-coordinate of center of fire (m)
	US(3)	·	z-coordinate of base of fire (m)

The SCEN card gives the observer and target positions in the user coordinate system. The positions must lie on opposite sides of the x-axis in the FITTE coordinate system.

Table 6. The SCEN card

Identifier SCEN	Variable	Default	Description LOS data
	UO(1)		observer x coordinate (m)
	UO(2)		observer y coordinate (m)
	UO(3)		observer z coordinate (m)
	UT(1)		target x coordinate (m)
	UT(2)		target y coordinate (m)
	UT(3)		target z coordinate (m)

Most of the input data for the METD card are self-explanatory. The wind direction is determined by the usual meteorological convention; the upwind direction measured clockwise from north. The Pasquill stability category has a range of 1 to 6, compared with the usual classification 1 = A, 2 = B, etc.

Table 7. The METD card

Identifier	Variable	Default	Description
METD			Meteorological data
	UBAR		mean ambient windspeed (m/s)
	WDIR		wind direction (meteorological convention, °)
	TAIR		ambient air temperature (°C)
	RH		relative humidity (%)
	RHO		ambient air density (g/m^3)
	IPAS		Pasquill stability category (range 1 to 6)

The DETD card specifies the initial laser beam diameter for a scenario 1 or 2 simulation. Use any convenient diameter because the model predicts beam magnification rather than diameter after propagation.

Table 8. The DETD card

Identifier	Variable	Default	Description
DETD			Laser data
	BEAM		beam diameter (cm)

Use the TARG card to obtain contrast data for a target with a temperature other than ambient for a scenario 1 or 2 situation.

Table 9. The TARG card

Identifier	Variable	Default	Description
TARG			Target data for thermal emission calculations
	TTARG		target temperature (°C)
	ETARG		target emissivity (dimensionless, range 0 to 1)

Use the MOLS card to specify inclusion of molecular effects in the radiance and transmittance calculations. It also controls whether the transmittance and radiance calculations are performed only through the plume, or if the effect of molecular absorption and emission in the atmosphere between plume and observer is included. The ambient carbon dioxide and water vapor concentrations are used in this calculation; other atmospheric gases are not included. If IATM is 1, the stepwise calculation through the plume is continued from the near plume edge to the observer position.

Table 10. The MOLS card

Identifier MOLS	Variable	Default	Description Molecular effects calculation control
	IMOL	1	flag for molecular transmittance calculation: 0 $\Rightarrow$ molecular transmittance not included 1 $\Rightarrow$ molecular transmittance included
	IATM	0	flag for calculations outside the plume: 0 $\Rightarrow$ omit calculations between observer and plume 1 $\Rightarrow$ include calculations between observer and plume

Use the BAND card to specify waveband calculations and to furnish parameters for their control. It also controls the instrument response function used for a waveband calculation. There are three instrument response functions from which to choose: a rectangle, a triangle, and a trapezoid. The code in subroutine RESPNS is written so other functions may be easily added, and the method for constructing instrument response functions is described in the source code. When a waveband calculation is performed for the FGLOW scenario, the aerosol optical properties used are for the center wavelength of the band. If the FGLOW output data are specified as apparent temperature, a blackbody equivalent temperature is calculated based on a conversion of the band-integrated radiation to a weighted average value at the center wavelength of the band.

Specify the beginning and ending wave numbers of the band and the number of calculation points in the band. The response function value is calculated for each of the points. The rectangle has values of 1 in the band, 0 outside the band, and 0.5 at the boundaries. The triangle has a peak of 1 and goes to 0 at the boundaries. The trapezoid is 0 at the boundaries, rises linearly from 0 to 1 over the outer 20 percent of the band on each side, and has a value of 1 for the central 60 percent of the band.

The number of calculation points in the band must be odd so a point is defined at the center of the band. The code checks for this and corrects it if necessary. If such a correction is made, the number of points (and therefore the wave number increment) differs from the user input.

Table 11. The BAND card

Identifier BAND	Variable	Default	Description Wave band calculation control
	IBAND	0	flag wave band calculations: 0 ⇒ single wavelength calculation 1 ⇒ perform wave band calculation
	WVN1		beginning wave number of band (cm^{-1})
	WVN2		ending wave number of band (cm^{-1})
	NWVN	1	number of wave number intervals in band (must be odd)
	IRESP	0	instrument response function over wave band: 0 - rectangular 1 - triangular 2 - trapezoidal
	IPSPEC	0	switch printing of spectrally resolved values: 0 ⇒ do not print resolved values 1 ⇒ print resolved transmittance and radiance values

The OPT1 card permits the user to override the default values of TCRITA, the fractional change in temperature that triggers calls to ATLESF; NUMINT, the number of calculation intervals through the plume (should be an even number);

and NUMSEG, the number of calculation intervals between the plume and observer. The default values speed calculations and give good results.

Table 12. The OPT1 card

Identifier OPT1	Variable	Default	Description Optional parameters for calculation control
	TCRITA	0.10	fractional change in temperature which triggers a call to the band model
	NUMINT	30	number of calculation steps through the plume
	NUMSEG	1	number of path segments for calculation from plume to observer

The SCN3 card supplies imager parameters needed for scenario 3 calculations and control. Although the option to produce apparent temperature output image data files has not been removed from the code, this option should not be used. Accessory programs, described in appendix B, can transform the radiance image data to apparent temperature image data.

Table 13. The SCN3 card

Identifier SCN3	Variable	Default	Description Imager parameters for scenario 3 (FGLOW)
	AINC		resolution per pixel (mrad)
	NGX		number of columns of pixels
	NGZ		number of rows of pixels
	IAPT	0	code for type of data stored: 0 $\Rightarrow$ radiance and transmittance data 1 $\Rightarrow$ apparent temperature data

Use the TCAL card to specify an internal time-series calculation. If FITTE is called by other modules within EOSAEL, only the output parameters from the final time are passed back to the calling routine. Time-series calculations suppress printing of waveband resolved output. All times are converted to integers because the built-in time constant for calculations is 1 s. The VEL0 parameter, normally, is zero, but it can be used to specify movement of the

observer toward the target along the LOS during the time series calculation. If the observer crosses the model system wind-aligned axis, the calculations are aborted and a message is written to the output file.

Table 14. The TCAL card

Identifier TCAL	Variable	Default	Description Time-series calculation control
	STIME	100	start time for calculations (seconds after start of fire)
	TINC	1	time increment between calculations (s)
	NCALC	1	number of calculations in time series
	VEL0	0	velocity of observer toward target along LOS (m/s)

The SVAR card lets the user modify certain fire parameters. It is, primarily, intended to permit matching of parameters for comparison with experimental data. USE THE SVAR CARD WITH CAUTION — IT CAN CAUSE UNREALISTIC COMBINATIONS OF FIRE PARAMETERS AND ERRONEOUS PREDICTIONS. You should monitor the value of vertical wind W_o printed in the output file when the fire parameters are varied. A value much outside the range 1.5 to 3 m/s indicates that the combined fire parameters have changed significantly from measured values and the model predictions may not be accurate. See appendix C for a discussion of varying the fire parameters and developing model fire parameters from data.

Table 15. The SVAR card

Identifier SVAR	Variable	Default	Description Variation of fire parameters
	TEMPIN	973.16	fire mean temperature (K)
	EFFAC	1	fractional multiplier of aerosol efficiency factor
	RADIN		radius of fire (m)
	BTIME	1500	burn time (s)

The mean fire temperature TEMPIN can be varied fairly freely. The current value seems to give accurate radiation temperature distributions for fires enclosed within metallic hulls. For open burning of fuel, the appropriate mean temperature may be up to several hundred degrees higher than the default value used in the model. If the variation of the fire parameters is performed to match experimental data, the peak temperature in the Gaussian plume at the fire is roughly 2.9 times the mean temperature.

EFFAC is a fractional multiplier that allows you to vary the creation of smoke aerosols. Normally, it is set to 1.0, but can be any number. Values between about 0.67 and 1.33 would cover the general range of smoke variation for hydrocarbon fuel fires.

RADIN allows you to vary the fire radius. Plume scaling in the atmosphere is generally considered to occur for fire diameters of no less than 1 m, so the minimum value for RADIN should be 0.5 m. Note that the actual fire image appears to have approximately two-thirds the specified source radius.

BTIME allows you to vary the total burn time for the fire. The current value is 1500 s (25 min). Large variations from this value are inappropriate for open burning conditions, but substantial increases might be called for to simulate an enclosed fire in which the burn rate is controlled by an inadequate oxygen supply.

Use the GO card to indicate that repetitive calculations are to be performed for which new parameter values are read between model runs.

Table 16. The GO card

Identifier	Variable	Default	Description
GO			Execute and read data for a subsequent run

Use the DONE card to execute a single run or the last of a series of runs. It returns control to the driver program.

Table 17. The DONE card

Identifier	Variable	Default	Description
DONE			Execute and return control to EOEXEC

The default values shown on the cards are used if no value is furnished. As can be seen, not all variables have default values. Other (default substitute) values are used when certain input parameters are outside an appropriate range of values. A notice that identifies the input card involved is printed in the output file if any substitution of values is made.

Selecting a turbulence effects calculation, a time-series calculation, or a scenario 3 (FGLOW) calculation (particularly for waveband calculations) may increase run time significantly. Typical run times on a 20-MHz 386 PC with coprocessor are shown in table 18.

Table 18. Run times for selected run conditions

single LOS	single wavelength	1 min	12 s
single LOS	25 wave number band	0 min	13 s
single LOS	single wavelength		
25 point time series	with turbulence effects	14 min	23 s
	without turbulence effects	0 min	34 s
single LOS	25 wave number band	1 min	2 s
25 point time series			
25 by 25 array	single wavelength	3 min	45 s
(625 total LOS)			
25 by 25 array	25 wave number band	39 min	28 s
(625 total LOS)			

4.2　Output

4.2.1　*Parameters Returned to the Calling Routine*

The parameters available for return to the calling routine were increased. They now include the following:

> FITRAN - the total transmittance for the LOS
> IERR　 - a code to indicate an invalid input card identifier
> ATRAD　- the attenuated target radiance for the LOS
> PATRAD - the emitted radiance from the plume for the LOS
> CONLEN - the aerosol concentration-length product for the LOS
> SPTMAG - the turbulence-induced spot (area) magnification
> JITRAD - the turbulence-induced beam wander radius.

All the parameters (except the error code) are output for scenario 1 or 2 calculations that include turbulence effects. If turbulence effects calculations are omitted, the last two parameter values are meaningless.

For FGLOW calculations, the output parameters are those for the LOS with the highest emitted radiance.

4.2.2　*Output Printed or Stored in Files*

FITTE scenario 1 or 2 output is contained in a single file. Samples are shown in the example section. Most of the input data are listed, plume parameters are given for the calculation point on the LOS closest to the plume centerline, and the model predictions are printed. The output parameters provided are modeled calculation time, total transmittance, aerosol transmittance, attenuated target radiance, emitted radiance, apparent temperature, concentration-length, and, for single wavelength calculations that include turbulence effects, laser spot magnification, and jitter radius.

If transmittance and radiance are calculated over a spectral band, you have the option (set IPSPEC = 1 on BAND) of printing the spectrally resolved values of the radiative transfer predictions. Quantities printed are the wavelength, wave number, transmittance, target radiance, emitted radiance, total radiance,

and instrument spectral response. You cannot exercise this option if a time-series or an FGLOW calculation is being performed.

For the FGLOW scenario, two output files are created. The standard output file contains a summary of input data and information about the matrix data file created. The second file created contains a header with information on calculation parameters and *ngx* times *ngz* rows that contain emitted radiance and total transmittance data or apparent temperature data for the image matrix specified on the SCN3 card. The examples show samples for running FITTE for various conditions. The output file is named FGLOW1.FDT for a single image calculation. If a time-series of *n* images is calculated, the files are named FGLOW1.FDT to FGLOWn.FDT. The FGLOW data files should be renamed if you wish to keep them because the model overwrites one (or more) of the files the next time it is run.

5. Sample Runs

This section shows examples for running FITTE for various conditions. The examples show the input card and output files and may be accompanied by comments, an FGLOW data file, and illustrations of FGLOW output.

The examples and output were current at the time the manual was prepared for publication. Some changes may occur because of code modifications. Check the sample input/output files from the EOSAEL tape to identify any such changes.

The examples were chosen to illustrate most of the model options and were run under the following conditions:

(1) The synthetic wind fluctuation file FITEX.DAT was copied to FIT4D.DAT. To obtain more realistic output, one of the wind fluctuation files based on field data (see information in the file README.FIT) should be copied to FIT4D.DAT after the examples are run.

(2) The input files listed are for use with the PC version of the code using FITDRV as the main program. Several additional cards are needed to use the EOSAEL main driver. The additional cards include a WAVL and a FITTE card as a minimum, and may include cards with climate and geometry data.

(3) The EOSAEL header page was omitted from the output files.

(4) The DONE, END, and STOP cards were omitted from most of the examples.

5.1 Example 1: A Scenario 1 Calculation for a Single Wavelength

The user coordinate system positive *x*-axis points east, and a type 2 fire is used for a scenario 1 calculation through a 4D plume. The target temperature is 10 °C and has an emissivity of 0.8. The initial laser beam diameter is 0.3 cm.

```
INPUT:   REFD    90.0     2.       1.       1.
         SCEN     8.0  -100.0      6.0      8.0     900.0     6.0
         DETD     0.30
         METD     3.0    270.      6.5     83.0    1200.0     3.0
         SRCD     0.0      0.0      0.0
         TARG    10.       0.8
         DONE
         END
         STOP

OUTPUT:
                          ******************
                          *   EOSAEL 92    *
                          * 4D FITTE INPUT *
                          ******************

                          FIRE TYPE: TRUCK

              X-AXIS HEADING:    90.0 DEG CW FROM NORTH

                   POSITION M  (    X   ,    Y    ,    Z   ) :
                   OBSERVER    (   8.0,  -100.0,    6.0 )
                   TARGET      (   8.0,   900.0,    6.0 )
                   FIRE        (   0.0,     0.0,    0.0 )

                          METEOROLOGICAL DATA :
             WINDSPEED      3.0 M/S      WIND DIRECTION     270.0 DEG
             TEMPERATURE    6.5 C        RELATIVE HUMIDITY   83.0 %
             AIR DENSITY  1200.0 G/M**3  PASQUILL CATEGORY    3

             TARGET TEMPERATURE  10.0 C          EMISSIVITY   0.80

             LASER WAVELENGTH   0.63 UM     BEAM DIAMETER   0.30 CM


                          PLUME CONSTANTS :
          VERTICAL WIND (WO)       2.39 M/S    COEFFICIENT (C)       6.906
          BUOYANCY FLUX (F)        37.5        VIRTUAL SOURCE POSITION (M)
          ENTRAINMENT CONSTANT     0.4134      XV:  -7.12, ZV:  -8.52


    PLUME-LOS GEOMETRIC AND DISTRIBUTION FUNCTION DATA AT CLOSEST APPROACH:

             CENTERLINE COORDINATES  (     7.26,    -0.12,    5.68 ) M
             LOS COORDINATES         (     8.00,    -0.24,    6.00 ) M
             DISTANCE        0.82 M     EXCESS TEMPERATURE      153. C
             PLUME RADIUS    2.32 M     AEROSOL DENSITY     0.25 G/M**3

                   ******************************
                   *    4D FITTE PREDICTIONS    *
                   ******************************
```

TIME	TRANSMITTANCE		ATTENUATED				SPOT	JITTER
	TOTAL	AEROSOL	TARG RAD	PATH RAD	APP TEMP	CL	MAGN	RADIUS
sec			watts/m**2/sr/um		kelvin	g/m**2		m
100.	0.00	0.00	0.129E-28	0.275E-15	403.0	1.25	11.6	0.00

5.2 Example 2: A Scenario 2 Calculation for a Single Wavelength

The only change from example 1 is that the calculation is done for scenario 2. Note the effect of reversing the direction of the calculation on the turbulence effects output.

```
INPUT:   REFD      90.0      2.        2.        1.
         SCEN       8.0    -100.0      6.0       8.0     900.0      6.0
         DETD       0.30
         METD       3.0     270.       6.5      83.0    1200.0      3.0
         SRCD       0.0      0.0       0.0
         TARG      10.       0.8

OUTPUT:
                              *******************
                              *   EOSAEL 92     *
                              * 4D FITTE INPUT *
                              *******************

                              FIRE TYPE: TRUCK

              X-AXIS HEADING:    90.0 DEG CW FROM NORTH

                   POSITION M  (    X   ,    Y    ,    Z   ) :
                   OBSERVER    (    8.0,  -100.0,    6.0 )
                   TARGET      (    8.0,   900.0,    6.0 )
                   FIRE        (    0.0,     0.0,    0.0 )

                         METEOROLOGICAL DATA :
             WINDSPEED        3.0 M/S      WIND DIRECTION      270.0 DEG
             TEMPERATURE      6.5 C        RELATIVE HUMIDITY    83.0 %
             AIR DENSITY   1200.0 G/M**3   PASQUILL CATEGORY      3

              TARGET TEMPERATURE  10.0 C              EMISSIVITY   0.80

              LASER WAVELENGTH   0.63 UM      BEAM DIAMETER   0.30 CM


                              PLUME CONSTANTS :
             VERTICAL WIND (WO)      2.39 M/S   COEFFICIENT (C)        6.906
             BUOYANCY FLUX (F)      37.5        VIRTUAL SOURCE POSITION (M)
             ENTRAINMENT CONSTANT   0.4134      XV:  -7.12,  ZV:  -8.52


       PLUME-LOS GEOMETRIC AND DISTRIBUTION FUNCTION DATA AT CLOSEST APPROACH:

                   CENTERLINE COORDINATES (    7.26,   -0.12,    5.68 ) M
                   LOS COORDINATES        (    8.00,   -0.24,    6.00 ) M
                   DISTANCE       0.82 M    EXCESS TEMPERATURE     153. C
                   PLUME RADIUS   2.32 M    AEROSOL DENSITY      0.25 G/M**3


                        ******************************
                        *    4D FITTE PREDICTIONS     *
                        ******************************
```

TIME sec	TRANSMITTANCE TOTAL	AEROSOL	ATTENUATED TARG RAD watts/m**2/sr/um	PATH RAD	APP TEMP kelvin	CL g/m**2	SPOT MAGN	JITTER RADIUS m
100.	0.00	0.00	0.129E-28	0.275E-15	403.0	1.25	1.0	0.00

5.3 Example 3: A Scenario 1 Calculation for a (Visible) Waveband

FITTE does not include molecular effects for this waveband.

```
INPUT:   REFD      90.0      2.        1.        1.
         SCEN       8.0   -100.0       6.0       8.0      900.0       6.0
         DETD       0.30
         METD       3.0     270.       6.5      83.0     1200.0       3.0
         SRCD       0.0       0.0      0.0
         TARG      10.        0.8
         BAND       1.    13000.    19231.      25.        2.         0.

OUTPUT:
```

```
                              ******************
                              *   EOSAEL 92     *
                              * 4D FITTE INPUT *
                              ******************

                              FIRE TYPE: TRUCK

                    X-AXIS HEADING:    90.0 DEG CW FROM NORTH

                    POSITION M  (    X  ,     Y  ,     Z   ) :
                    OBSERVER    (    8.0,  -100.0,    6.0 )
                    TARGET      (    8.0,   900.0,    6.0 )
                    FIRE        (    0.0,     0.0,    0.0 )

                              METEOROLOGICAL DATA :
              WINDSPEED       3.0 M/S       WIND DIRECTION     270.0 DEG
              TEMPERATURE     6.5 C         RELATIVE HUMIDITY   83.0 %
              AIR DENSITY  1200.0 G/M**3    PASQUILL CATEGORY    3

                  TARGET TEMPERATURE  10.0 C              EMISSIVITY   0.80

                              WAVEBAND DATA :
       WAVEBAND FROM 13000.00 CM-1  TO  19231.00 CM-1    CENTER WAVELENGTH   0.621 UM
       25 POINTS RESOLUTION        INSTRUMENT RESPONSE: TRAP     MOLECULES INCLUDED: YES
                      WAVEBAND DOES NOT OVERLAP FITTE MOLECULAR DATA

                              PLUME CONSTANTS :
              VERTICAL WIND (WO)      2.39 M/S   COEFFICIENT (C)        6.906
              BUOYANCY FLUX (F)       37.5       VIRTUAL SOURCE POSITION (M)
              ENTRAINMENT CONSTANT    0.4134     XV:  -7.12,  ZV:  -8.52

       PLUME-LOS GEOMETRIC AND DISTRIBUTION FUNCTION DATA AT CLOSEST APPROACH:

              CENTERLINE COORDINATES  (    7.26,    -0.12,    5.68 ) M
              LOS COORDINATES         (    8.00,    -0.24,    6.00 ) M
              DISTANCE        0.82 M      EXCESS TEMPERATURE      153. C
              PLUME RADIUS    2.32 M      AEROSOL DENSITY      0.25 G/M**3

                    ******************************
                    *    4D FITTE PREDICTIONS     *
                    ******************************
```

```
         TRANSMITTANCE    ATTENUATED
  TIME   TOTAL  AEROSOL   TARG RAD    PATH RAD    APP TEMP    CL
  sec                        watts/m**2/sr         kelvin   g/m**2

  100.   0.00    0.00    0.283E-36    0.860E-14    448.5     1.25
```

66

5.4 Example 4: A Scenario 1 Time-Series Calculation for a Single Wavelength

The TCAL card specifies a time-series calculation. The calculation starts 100 s after the start of the fire. The interval between calculations is 1 s, and 11 calculations are performed to span a 10-s period. At this wavelength (1.06 μm), the inclusion of molecular absorption has no effect on the transmittance.

```
INPUT:   REFD    90.000    3.000    1.      1.
         SCEN     5.000  400.000    3.00    5.000  -800.000    3.0
         SRCD     0.000    0.000    0.000
         DETD     5.000
         TARG    37.0      1.0
         METD     4.000  270.000   27.000   60.000  1009.728    4.000
         TCAL   100.       1.      11.       0.
         MOLS     1.       1.
```

OUTPUT:

```
                        ******************
                        *   EOSAEL 92    *
                        * 4D FITTE INPUT *
                        ******************

                          FIRE TYPE: TANK

                X-AXIS HEADING:    90.0 DEG CW FROM NORTH

                POSITION M (    X   ,    Y    ,    Z   ) :
                OBSERVER   (    5.0,   400.0,    3.0 )
                TARGET     (    5.0,  -800.0,    3.0 )
                FIRE       (    0.0,     0.0,    0.0 )

                         METEOROLOGICAL DATA :
        WINDSPEED        4.0 M/S      WIND DIRECTION      270.0 DEG
        TEMPERATURE     27.0 C        RELATIVE HUMIDITY    60.0 %
        AIR DENSITY   1009.7 G/M**3   PASQUILL CATEGORY     4

        TARGET TEMPERATURE  37.0 C              EMISSIVITY   1.00

        LASER WAVELENGTH  1.06 UM      BEAM DIAMETER   5.00 CM


                         PLUME CONSTANTS :
        VERTICAL WIND (WO)     2.78 M/S    COEFFICIENT (C)        10.887
        BUOYANCY FLUX (F)    169.1         VIRTUAL SOURCE POSITION (M)
        ENTRAINMENT CONSTANT   0.4433      XV: -17.71, ZV: -18.49


    PLUME-LOS GEOMETRIC AND DISTRIBUTION FUNCTION DATA AT CLOSEST APPROACH:

            CENTERLINE COORDINATES (    3.87,   -0.52,    3.24 ) M
            LOS COORDINATES        (    5.00,   -0.50,    3.00 ) M
            DISTANCE      1.15 M    EXCESS TEMPERATURE       0. C
            PLUME RADIUS  2.87 M    AEROSOL DENSITY      1.28 G/M**3
```

```
******************************
*    4D FITTE PREDICTIONS    *
******************************
```

FITTE OUTPUT FOR TIME-SERIES CALCULATION

TIME sec	TRANSMITTANCE TOTAL	AEROSOL	ATTENUATED TARG RAD watts/m**2/sr/um	PATH RAD	APP TEMP kelvin	CL g/m**2	SPOT MAGN	JITTER RADIUS m
100.	0.00	0.00	0.107E-14	0.296E-01	622.6	3.05	172.4	0.44
101.	0.00	0.00	0.446E-14	0.321E+01	792.9	2.56	224.9	0.49
102.	0.00	0.00	0.317E-17	0.157E+00	674.2	5.03	477.0	0.66
103.	0.00	0.00	0.278E-13	0.134E-03	499.1	1.94	80.6	0.32
104.	0.00	0.00	0.250E-15	0.304E+00	697.0	3.54	539.4	0.69
105.	0.00	0.00	0.832E-15	0.596E+00	721.9	3.14	327.5	0.56
106.	0.00	0.00	0.171E-15	0.707E-01	648.5	3.67	291.5	0.54
107.	0.05	0.05	0.409E-12	0.148E-04	461.8	1.03	49.6	0.26
108.	0.06	0.06	0.530E-12	0.159E-04	462.9	0.94	61.6	0.29
109.	0.03	0.03	0.240E-12	0.688E-03	531.1	1.21	70.9	0.30
110.	0.00	0.00	0.727E-14	0.865E+00	736.5	2.40	340.0	0.57

5.5 Example 5: A Scenario 1 Calculation With Variation of Fire Parameters and Printout of Spectrally Resolved Results for a Selected Instrument Response Function

This calculation is performed over an IR waveband. The last two parameters on the BAND card specify use of a trapezoidal response function and printout of spectrally resolved output. Note the use of the SVAR card to specify a higher fire temperature.

```
INPUT:    REFD      90.0      2.        1.       1.
          SCEN       0.0      0.0       80.0     30.0    1800.0    20.0
          DETD       0.30
          METD       3.0      255.      6.5      83.0    1200.0     3.0
          SRCD      -6.0     1650.0     0.0
          TARG      10.        0.8
          SVAR     1223.       1.
          BAND       1.      2600.     3300.     25.       2.        1.

OUTPUT:
```

```
                     ******************
                     *   EOSAEL 92    *
                     * 4D FITTE INPUT *
                     ******************

                       FIRE TYPE: TRUCK
                   USER ENTERED FIRE VARIATION:
                   AVERAGE TEMPERATURE:   1223. K

           X-AXIS HEADING:      90.0 DEG CW FROM NORTH

               POSITION M  (    X    ,    Y    ,    Z   ) :
               OBSERVER    (    0.0,      0.0,     80.0 )
               TARGET      (   30.0,   1800.0,     20.0 )
               FIRE        (   -6.0,   1650.0,      0.0 )

                       METEOROLOGICAL DATA :
          WINDSPEED        3.0 M/S     WIND DIRECTION      255.0 DEG
          TEMPERATURE      6.5 C       RELATIVE HUMIDITY    83.0 %
          AIR DENSITY   1200.0 G/M**3  PASQUILL CATEGORY     3

          TARGET TEMPERATURE  10.0 C             EMISSIVITY   0.80

                          WAVEBAND DATA :
          WAVEBAND FROM  2600.00 CM-1  TO  3300.00 CM-1    CENTER WAVELENGTH    3.390 UM
          25 POINTS RESOLUTION      INSTRUMENT RESPONSE: TRAP      MOLECULES INCLUDED: YES

                          PLUME CONSTANTS :
          VERTICAL WIND (WO)     2.16 M/S   COEFFICIENT (C)         6.666
          BUOYANCY FLUX (F)      37.5       VIRTUAL SOURCE POSITION (M)
          ENTRAINMENT CONSTANT   0.4359     XV:  -8.68,  ZV:  -9.38

          PLUME-LOS GEOMETRIC AND DISTRIBUTION FUNCTION DATA AT CLOSEST APPROACH:

               CENTERLINE COORDINATES  (    25.81,   1657.55,    19.09 ) M
               LOS COORDINATES         (    27.65,   1659.16,    24.69 ) M
               DISTANCE        6.12 M   EXCESS TEMPERATURE          0. C
               PLUME RADIUS    7.24 M   AEROSOL DENSITY        0.00 G/M**3
```

```
*****************************
*    4D FITTE PREDICTIONS    *
*****************************
```

TIME sec	TRANSMITTANCE TOTAL	AEROSOL	ATTENUATED TARG RAD	PATH RAD watts/m**2/sr	APP TEMP kelvin	CL g/m**2
100.	0.85	0.85	0.105E-01	0.714E-02	263.9	0.12

SPECTRAL RADIANCE AND TRANSMITTANCE

WAVELTH (UM)	FREQ (CM**-1)	TRANS	TARG RAD	PATH RAD (WATTS/M**2/SR/CM)	TOTAL RAD	INSTR RESPONSE
3.8462	2600.000	0.8556	2.423E-05	4.050E-05	6.473E-05	0.0000
3.8035	2629.167	0.8552	2.369E-05	3.616E-05	5.984E-05	0.2083
3.7618	2658.333	0.8544	2.315E-05	3.237E-05	5.552E-05	0.4167
3.7209	2687.500	0.8535	2.262E-05	2.897E-05	5.160E-05	0.6250
3.6810	2716.667	0.8527	2.212E-05	2.592E-05	4.804E-05	0.8333
3.6419	2745.833	0.8519	2.163E-05	2.318E-05	4.481E-05	1.0000
3.6036	2775.000	0.8511	2.116E-05	2.071E-05	4.187E-05	1.0000
3.5661	2804.167	0.8503	2.070E-05	1.850E-05	3.921E-05	1.0000
3.5294	2833.333	0.8496	2.026E-05	1.652E-05	3.678E-05	1.0000
3.4934	2862.500	0.8488	1.983E-05	1.475E-05	3.458E-05	1.0000
3.4582	2891.667	0.8481	1.942E-05	1.316E-05	3.257E-05	1.0000
3.4237	2920.833	0.8474	1.902E-05	1.173E-05	3.075E-05	1.0000
3.3898	2950.000	0.8467	1.863E-05	1.046E-05	2.908E-05	1.0000
3.3566	2979.167	0.8460	1.825E-05	9.319E-06	2.757E-05	1.0000
3.3241	3008.333	0.8453	1.788E-05	8.300E-06	2.618E-05	1.0000
3.2922	3037.500	0.8447	1.753E-05	7.390E-06	2.492E-05	1.0000
3.2609	3066.667	0.8440	1.718E-05	6.578E-06	2.376E-05	1.0000
3.2301	3095.833	0.8434	1.685E-05	5.852E-06	2.270E-05	1.0000
3.2000	3125.000	0.8428	1.652E-05	5.205E-06	2.173E-05	1.0000
3.1704	3154.167	0.8422	1.621E-05	4.628E-06	2.083E-05	1.0000
3.1414	3183.333	0.8416	1.590E-05	4.113E-06	2.001E-05	0.8333
3.1128	3212.500	0.8410	1.560E-05	3.655E-06	1.926E-05	0.6250
3.0848	3241.667	0.8404	1.531E-05	3.246E-06	1.856E-05	0.4167
3.0573	3270.833	0.8399	1.503E-05	2.883E-06	1.791E-05	0.2083
3.0303	3300.000	0.8393	1.476E-05	2.559E-06	1.731E-05	0.0000

5.6 Example 6: A Single Wavelength Scenario 3 Calculation

The SCN3 card provides all parameters except wavelength and waveband for the scenario 3 imager. The angular resolution is 0.5 mrad per pixel. A 5-column, 3-row array of radiance and temperature is stored after the parameter summary line in the data file (shown on the next page). The pixel size is large enough, compared with the plume width, that the values in the data array are area averaged. The -1 on the REFD card specifies a mean-value plume. The FGLOW1.FDT file is shown on the next page.

```
INPUT:   REFD      90.000    2.000    3.       -1.
         SCEN      25.000 -1000.000   20.00    25.000   100.000   20.0
         SRCD       0.000     0.000    0.000
         METD       3.000   270.000   27.000   60.000  1009.728    4.000
         SCN3       0.50      5.       3.       0.

OUTPUT:
                        ******************
                        *   EOSAEL 92    *
                        * 4D FITTE INPUT *
                        ******************

                           FIRE TYPE: TRUCK

                    X-AXIS HEADING:    90.0 DEG CW FROM NORTH

                      POSITION M (    X   ,    Y   ,    Z   ) :
                      OBSERVER  (   25.0, -1000.0,   20.0 )
                      TARGET    (   25.0,   100.0,   20.0 )
                      FIRE      (    0.0,     0.0,    0.0 )

                         METEOROLOGICAL DATA :
                 WINDSPEED      3.0 M/S      WIND DIRECTION    270.0 DEG
                 TEMPERATURE   27.0 C        RELATIVE HUMIDITY  60.0 %
                 AIR DENSITY  1009.7 G/M**3  PASQUILL CATEGORY   4

                             IMAGER DATA:
              TOTAL FOV:   2.50 BY   1.50 (MR)    RESOLUTION PER PIXEL 0.50 MR
                         PIXELS (HORIZONTAL, VERTICAL) (  5,  3 )
                             WAVELENGTH  10.60 UM


                           PLUME CONSTANTS :
              VERTICAL WIND (WO)     2.74 M/S   COEFFICIENT (C)      7.530
              BUOYANCY FLUX (F)      41.5       VIRTUAL SOURCE POSITION (M)
              ENTRAINMENT CONSTANT   0.3820     XV:  -6.17,  ZV:  -8.45

                         ****************
                         * FGLOW OUTPUT *
                         ****************
                    AT 100. SECONDS AFTER START OF FIRE

          RADIANCE AND TRANSMITTANCE DATA STORED FOR   5 COLUMN,   3 ROW ARRAY.
          THE TOP LEFT CORNER PIXEL IS AT (   24.00,    0.00,   20.50 ) M
          AND THE ARRAY CENTER IS AT      (   25.00,    0.00,   20.00 ) M
          IN A PLANE ( PERPENDICULAR TO THE LOS AND AT THE SOURCE DISTANCE
          FROM THE OBSERVER ) IN THE USER COORDINATE SYSTEM.
          POINT SPACING IS   0.500 M       UNITS: Watts/m**2/sr/um

                         VALUES ARE AREA AVERAGED
```

The data file is listed below. The first row contains the following information:

- the (single or center-of-waveband) wavelength for the calculation
- the number of columns and rows of imager data
- the coordinates of the center of the upper left pixel in the plane of the fire
- the angular resolution for one pixel
- the coordinates of the center pixel in the array
- the ambient temperature
- a waveband function (used to convert waveband integrated radiance to a single-wavelength blackbody equivalent temperature).

The succeeding rows each contain (radiance and transmittance) data for one pixel.

```
 10.60000   5   3   24.000     0.000   20.500    0.500   25.000     0.000   20.000 300.16 1.00
2.071363E+00     0.774
2.438133E+00     0.738
2.823721E+00     0.701
3.216068E+00     0.666
3.610541E+00     0.631
2.705834E+00     0.713
3.116120E+00     0.675
3.534536E+00     0.638
3.946305E+00     0.603
4.343624E+00     0.571
3.436608E+00     0.648
3.874342E+00     0.611
4.302427E+00     0.576
4.709477E+00     0.544
5.090297E+00     0.515
```

5.7   Example 7: A Scenario 3 Waveband Calculation

For this example, the calculation is done for a mean-value plume. The fourth parameter on the SCN3 card is set to 1 to produce apparent temperature rather than radiance and transmittance output. The FGLOW1.FDT file is shown on the next page. See example 6 for a description of the information included in the file.

This is no longer a recommended mode of operation. Unless apparent temperature information is the only information desired, it is more efficient to create a radiance and transmittance file and process it with the accessory programs described in appendix B to obtain apparent temperature output.

```
INPUT:    REFD      90.000     2.000      3.       -1.
          SCEN      25.000 -1000.000     20.00     25.000    100.000     20.0
          SRCD       0.000     0.000      0.000
          METD       3.000   270.000     27.000    60.000   1009.728      4.000
          SCN3       0.50      5.         3.        1.
          BAND       1.      793.65    1162.79     15.        2.          0.


OUTPUT:
                              *******************
                              *    EOSAEL 92    *
                              * 4D FITTE INPUT  *
                              *******************

                              FIRE TYPE: TRUCK

                  X-AXIS HEADING:    90.0 DEG CW FROM NORTH

                  POSITION M (   X   ,    Y   ,    Z   ) :
                  OBSERVER   (   25.0, -1000.0,    20.0 )
                  TARGET     (   25.0,   100.0,    20.0 )
                  FIRE       (    0.0,     0.0,     0.0 )

                         METEOROLOGICAL DATA :
              WINDSPEED        3.0 M/S      WIND DIRECTION      270.0 DEG
              TEMPERATURE     27.0 C        RELATIVE HUMIDITY    60.0 %
              AIR DENSITY   1009.7 G/M**3   PASQUILL CATEGORY     4

                              IMAGER DATA:
          TOTAL FOV:   2.50 BY   1.50 (MR)    RESOLUTION PER PIXEL 0.50 MR
                    PIXELS (HORIZONTAL, VERTICAL) (   5,   3 )
          WAVEBAND FROM   793.65 CM-1 TO  1162.79 CM-1    CENTER WAVELENGTH    10.223 UM
          15 POINTS RESOLUTION      INSTRUMENT RESPONSE: TRAP     MOLECULES INCLUDED: YES
                    APPARENT TEMPERATURE CALCULATED FOR CENTER WAVELENGTH


                              PLUME CONSTANTS :
              VERTICAL WIND (WO)    2.74 M/S   COEFFICIENT (C)        7.530
              BUOYANCY FLUX (F)    41.5        VIRTUAL SOURCE POSITION (M)
              ENTRAINMENT CONSTANT  0.3820     XV:  -6.17,  ZV:  -8.45
```

```
                        ****************
                        * FGLOW OUTPUT *
                        ****************
                  AT 100. SECONDS AFTER START OF FIRE

        APPARENT TEMPERATURE DATA STORED FOR    5 COLUMN,   3 ROW ARRAY.
        THE TOP LEFT CORNER PIXEL IS AT (    24.00,     0.00,    20.50 ) M
        AND THE ARRAY CENTER IS AT       (    25.00,     0.00,    20.00 ) M
        IN A PLANE ( PERPENDICULAR TO THE LOS AND AT THE SOURCE DISTANCE
        FROM THE OBSERVER ) IN THE USER COORDINATE SYSTEM.
        POINT SPACING IS    0.500 M        UNITS: degrees K

                        VALUES ARE AREA AVERAGED
```

The FGLOW1.FDT file is shown below.

```
10.22265   5   3   24.000     0.000    20.500     0.500    25.000     0.000    20.000 300.16 0.31
    299.
    299.
    299.
    299.
    299.
    299.
    299.
    299.
    300.
    300.
    299.
    300.
    300.
    301.
    301.
```

5.8 Example 8: A Time-Series of Single Wavelength Scenario 3 Calculations

The SCN3 and TCAL cards are used to create a sequence of images. The output data files, FGLOW1.FDT through FGLOW6.FDT, are not shown for this example. The output creates a series of files separated by 1 min that span a 5-min period. Figures 10a and b show contour plots of the data. The accessory program XS2GRD was used to transform the data files to input files for the plotting program.

```
INPUT:    REFD      90.0      2.        3.       1.
          SCEN       5.0   -1000.0      6.0      5.0     100.0      6.0
          SRCD       0.0      0.0       0.0
          METD       3.0    270.0      27.0     60.0    1009.728    4.0
          DETD       0.125
          TARG      10.0      0.8
          SCN3       0.125   121.      81.       0.
          TCAL     100.      60.        6.       0.

OUTPUT:

                          ******************
                          *   EOSAEL 92    *
                          * 4D FITTE INPUT *
                          ******************

                          FIRE TYPE: TRUCK

                X-AXIS HEADING:    90.0 DEG CW FROM NORTH

                POSITION M (    X  ,    Y   ,    Z   ) :
                OBSERVER   (    5.0, -1000.0,    6.0 )
                TARGET     (    5.0,   100.0,    6.0 )
                FIRE       (    0.0,     0.0,    0.0 )

                        METEOROLOGICAL DATA :
        WINDSPEED        3.0 M/S     WIND DIRECTION      270.0 DEG
        TEMPERATURE     27.0 C       RELATIVE HUMIDITY    60.0 %
        AIR DENSITY   1009.7 G/M**3  PASQUILL CATEGORY     4

                            IMAGER DATA:
        TOTAL FOV:  15.13 BY  10.13 (MR)   RESOLUTION PER PIXEL 0.13 MR
                    PIXELS (HORIZONTAL, VERTICAL) ( 121,  81 )
                           WAVELENGTH  10.60 UM

                        PLUME CONSTANTS :
        VERTICAL WIND (WO)     2.74 M/S   COEFFICIENT (C)        7.530
        BUOYANCY FLUX (F)      41.5       VIRTUAL SOURCE POSITION (M)
        ENTRAINMENT CONSTANT   0.3820     XV:  -6.17, ZV:  -8.45

                        ****************
                        * FGLOW OUTPUT *
                        ****************
                AT 100. SECONDS AFTER START OF FIRE

        RADIANCE AND TRANSMITTANCE DATA STORED FOR 121 COLUMN,  81 ROW ARRAY.
        THE TOP LEFT CORNER PIXEL IS AT (   -2.50,    0.00,   11.00 ) M
        AND THE ARRAY CENTER IS AT      (    5.00,    0.00,    6.00 ) M
        IN A PLANE ( PERPENDICULAR TO THE LOS AND AT THE SOURCE DISTANCE
        FROM THE OBSERVER ) IN THE USER COORDINATE SYSTEM.
        POINT SPACING IS    0.125 M        UNITS: Watts/m**2/sr/um
                    THIS WAS REPEATED   6 TIMES AT  60 SECOND INTERVALS
```
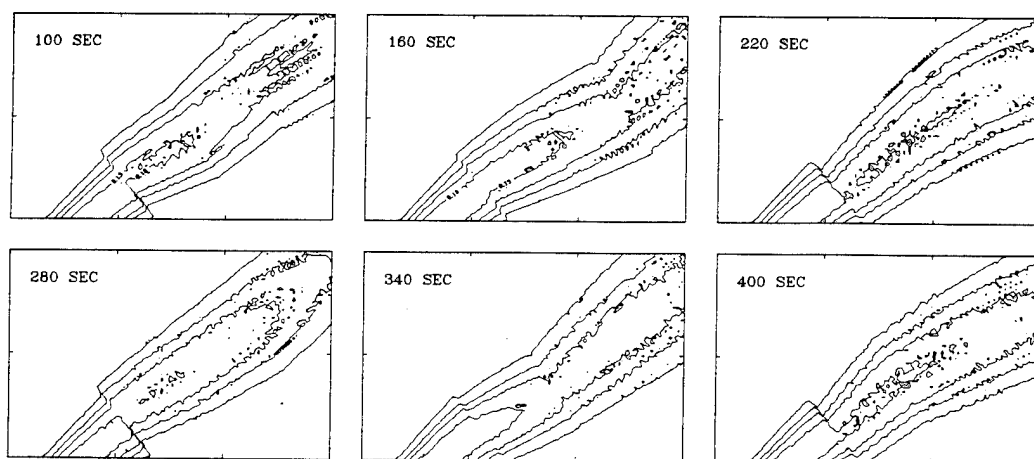
Figure 10a. Transmittance plots created with data from the example 8 simulation. Wavelength was 10.6 μm. Tic spacing is 5 m.
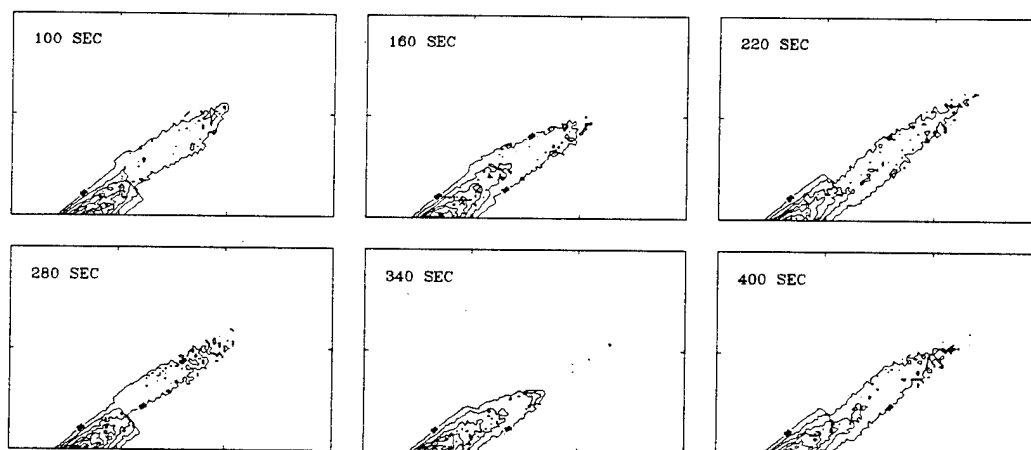
Figure 10b. Radiance plots created with data from the example 8 simulation. Wavelength was 10.6 μm. Tic spacing is 5 m.

5.9 Example 9: Internal Cycling With Variation of Wind Direction to Produce Five Output Files

Example 9 illustrates the use of the GO and DONE cards to perform a series of calculations with variation of parameters other than time. The five pages of the EX9.OUT file are shown. Figure 11 was prepared from the five (FGLOWn.FDT) data files. The accessory program XS2GRD transformed the data files to produce apparent temperature output files for the plotting program.

```
INPUT:    REFD     90.000      2.000     3.       1.
          SCEN      5.000  -1000.000     5.00     5.000    100.000    5.0
          SRCD      0.000      0.000     0.000
          METD      3.000    330.000    27.000    60.000   1009.728   4.000
          SCN3      0.125    121.       81.       0.
          GO
          METD      3.000    300.000    27.000    60.000   1009.728   4.000
          GO
          METD      3.000    270.000    27.000    60.000   1009.728   4.000
          GO
          METD      3.000    240.000    27.000    60.000   1009.728   4.000
          GO
          METD      3.000    210.000    27.000    60.000   1009.728   4.000
          DONE
```

OUTPUT:

```
                         ********************
                         *   EOSAEL 92     *
                         * 4D FITTE INPUT *
                         ********************

                         FIRE TYPE: TRUCK

            X-AXIS HEADING:    90.0 DEG CW FROM NORTH

              POSITION M  (    X   ,    Y    ,    Z   ) :
              OBSERVER    (    5.0, -1000.0,    5.0 )
              TARGET      (    5.0,   100.0,    5.0 )
              FIRE        (    0.0,     0.0,    0.0 )

                       METEOROLOGICAL DATA :
          WINDSPEED       3.0 M/S      WIND DIRECTION      330.0 DEG
          TEMPERATURE    27.0 C        RELATIVE HUMIDITY    60.0 %
          AIR DENSITY  1009.7 G/M**3   PASQUILL CATEGORY     4

                          IMAGER DATA:
        TOTAL FOV:  15.13 BY  10.13 (MR)    RESOLUTION PER PIXEL 0.13 MR
                  PIXELS (HORIZONTAL, VERTICAL)  ( 121,  81 )
                          WAVELENGTH   3.60 UM


                       PLUME CONSTANTS :
          VERTICAL WIND (WO)      2.74 M/S    COEFFICIENT (C)       7.530
          BUOYANCY FLUX (F)      41.5         VIRTUAL SOURCE POSITION (M)
          ENTRAINMENT CONSTANT   0.3820       XV:  -6.17, ZV:  -8.45

                       ****************
                       * FGLOW OUTPUT *
                       ****************
              AT 100. SECONDS AFTER START OF FIRE

    RADIANCE AND TRANSMITTANCE DATA STORED FOR 121 COLUMN,  81 ROW ARRAY.
    THE TOP LEFT CORNER PIXEL IS AT (    -2.50,     0.00,    10.00 ) M
    AND THE ARRAY CENTER IS AT      (     5.00,     0.00,     5.00 ) M
    IN A PLANE ( PERPENDICULAR TO THE LOS AND AT THE SOURCE DISTANCE
    FROM THE OBSERVER ) IN THE USER COORDINATE SYSTEM.
    POINT SPACING IS     0.125 M         UNITS: Watts/m**2/sr/um
```

```
******************
*   EOSAEL 92    *
* 4D FITTE INPUT *
******************


              FIRE TYPE: TRUCK

        X-AXIS HEADING:    90.0 DEG CW FROM NORTH


           POSITION M (    X   ,    Y    ,    Z   ) :
           OBSERVER   (    5.0, -1000.0,    5.0 )
           TARGET     (    5.0,   100.0,    5.0 )
           FIRE       (    0.0,     0.0,    0.0 )


                    METEOROLOGICAL DATA :
         WINDSPEED       3.0 M/S     WIND DIRECTION    300.0 DEG
         TEMPERATURE    27.0 C       RELATIVE HUMIDITY  60.0 %
         AIR DENSITY  1009.7 G/M**3  PASQUILL CATEGORY   4

                        IMAGER DATA:
         TOTAL FOV:  15.13 BY  10.13 (MR)    RESOLUTION PER PIXEL 0.13 MR
                  PIXELS (HORIZONTAL, VERTICAL)  ( 121,  81 )
                         WAVELENGTH   3.60 UM



                    PLUME CONSTANTS :
         VERTICAL WIND (WO)    2.74 M/S    COEFFICIENT (C)        7.530
         BUOYANCY FLUX (F)     41.5        VIRTUAL SOURCE POSITION (M)
         ENTRAINMENT CONSTANT  0.3820      XV:  -6.17, ZV:  -8.45


                    ******************
                    * FGLOW OUTPUT *
                    ******************
              AT 100. SECONDS AFTER START OF FIRE


RADIANCE AND TRANSMITTANCE DATA STORED FOR 121 COLUMN,  81 ROW ARRAY.
THE TOP LEFT CORNER PIXEL IS AT (     -2.50,      0.00,     10.00 ) M
AND THE ARRAY CENTER IS AT      (      5.00,      0.00,      5.00 ) M
IN A PLANE ( PERPENDICULAR TO THE LOS AND AT THE SOURCE DISTANCE
FROM THE OBSERVER ) IN THE USER COORDINATE SYSTEM.
POINT SPACING IS    0.125 M        UNITS: Watts/m**2/sr/um
```

```
                    ********************
                    *    EOSAEL 92     *
                    * 4D FITTE INPUT *
                    ********************

                      FIRE TYPE: TRUCK

          X-AXIS HEADING:    90.0 DEG CW FROM NORTH

          POSITION M (    X   ,    Y    ,    Z   ) :
          OBSERVER    (    5.0, -1000.0,    5.0 )
          TARGET      (    5.0,   100.0,    5.0 )
          FIRE        (    0.0,     0.0,    0.0 )


                    METEOROLOGICAL DATA :
     WINDSPEED        3.0 M/S    WIND DIRECTION     270.0 DEG
     TEMPERATURE     27.0 C      RELATIVE HUMIDITY   60.0 %
     AIR DENSITY   1009.7 G/M**3 PASQUILL CATEGORY    4

                        IMAGER DATA:
     TOTAL FOV:   15.13 BY  10.13 (MR)    RESOLUTION PER PIXEL 0.13 MR
              PIXELS (HORIZONTAL, VERTICAL) ( 121,  81 )
                      WAVELENGTH   3.60 UM



                    PLUME CONSTANTS :
     VERTICAL WIND (WO)    2.74 M/S   COEFFICIENT (C)        7.530
     BUOYANCY FLUX (F)     41.5       VIRTUAL SOURCE POSITION (M)
     ENTRAINMENT CONSTANT  0.3820     XV:  -6.17, ZV:  -8.45

                    ****************
                    * FGLOW OUTPUT *
                    ****************
              AT 100. SECONDS AFTER START OF FIRE

     RADIANCE AND TRANSMITTANCE DATA STORED FOR 121 COLUMN,  81 ROW ARRAY.
     THE TOP LEFT CORNER PIXEL IS AT (    -2.50,     0.00,    10.00 ) M
     AND THE ARRAY CENTER IS AT      (     5.00,     0.00,     5.00 ) M
     IN A PLANE ( PERPENDICULAR TO THE LOS AND AT THE SOURCE DISTANCE
     FROM THE OBSERVER ) IN THE USER COORDINATE SYSTEM.
     POINT SPACING IS    0.125 M       UNITS: Watts/m**2/sr/um
```

```
********************
*   EOSAEL 92    *
* 4D FITTE INPUT *
********************


            FIRE TYPE: TRUCK

     X-AXIS HEADING:    90.0 DEG CW FROM NORTH

        POSITION M  (    X    ,     Y    ,    Z  ) :
        OBSERVER    (    5.0, -1000.0,     5.0 )
        TARGET      (    5.0,   100.0,     5.0 )
        FIRE        (    0.0,     0.0,     0.0 )

                METEOROLOGICAL DATA :
     WINDSPEED       3.0 M/S     WIND DIRECTION      240.0 DEG
     TEMPERATURE    27.0 C       RELATIVE HUMIDITY    60.0 %
     AIR DENSITY  1009.7 G/M**3  PASQUILL CATEGORY     4

                    IMAGER DATA:
    TOTAL FOV:  15.13 BY  10.13 (MR)    RESOLUTION PER PIXEL 0.13 MR
            PIXELS (HORIZONTAL, VERTICAL) ( 121,  81 )
                    WAVELENGTH   3.60 UM


                PLUME CONSTANTS :
     VERTICAL WIND (WO)    2.74 M/S   COEFFICIENT (C)        7.530
     BUOYANCY FLUX (F)    41.5        VIRTUAL SOURCE POSITION (M)
     ENTRAINMENT CONSTANT  0.3820     XV:  -6.17, ZV:   -8.45

                ****************
                * FGLOW OUTPUT *
                ****************
            AT 100. SECONDS AFTER START OF FIRE


RADIANCE AND TRANSMITTANCE DATA STORED FOR 121 COLUMN,  81 ROW ARRAY.
THE TOP LEFT CORNER PIXEL IS AT (   -2.50,     0.00,    10.00 ) M
AND THE ARRAY CENTER IS AT      (    5.00,     0.00,     5.00 ) M
IN A PLANE ( PERPENDICULAR TO THE LOS AND AT THE SOURCE DISTANCE
FROM THE OBSERVER ) IN THE USER COORDINATE SYSTEM.
POINT SPACING IS    0.125 M       UNITS: Watts/m**2/sr/um
```

```
******************
*   EOSAEL 92    *
* 4D FITTE INPUT *
******************
```

FIRE TYPE: TRUCK

X-AXIS HEADING: 90.0 DEG CW FROM NORTH

```
        POSITION M  (    X   ,    Y    ,    Z  ) :
        OBSERVER    (    5.0, -1000.0,    5.0 )
        TARGET      (    5.0,   100.0,    5.0 )
        FIRE        (    0.0,     0.0,    0.0 )
```

METEOROLOGICAL DATA :

```
WINDSPEED        3.0 M/S     WIND DIRECTION      210.0 DEG
TEMPERATURE     27.0 C       RELATIVE HUMIDITY   60.0 %
AIR DENSITY   1009.7 G/M**3  PASQUILL CATEGORY    4
```

IMAGER DATA:

```
TOTAL FOV:  15.13 BY  10.13 (MR)    RESOLUTION PER PIXEL 0.13 MR
          PIXELS (HORIZONTAL, VERTICAL) ( 121,  81 )
                    WAVELENGTH   3.60 UM
```

PLUME CONSTANTS :

```
VERTICAL WIND (WO)      2.74 M/S    COEFFICIENT (C)        7.530
BUOYANCY FLUX (F)       41.5        VIRTUAL SOURCE POSITION (M)
ENTRAINMENT CONSTANT    0.3820      XV:  -6.17, ZV:  -8.45
```

```
****************
* FGLOW OUTPUT *
****************
```

AT 100. SECONDS AFTER START OF FIRE

```
RADIANCE AND TRANSMITTANCE DATA STORED FOR 121 COLUMN,  81 ROW ARRAY.
THE TOP LEFT CORNER PIXEL IS AT (    -2.50,     0.00,    10.00 ) M
AND THE ARRAY CENTER IS AT      (     5.00,     0.00,     5.00 ) M
IN A PLANE ( PERPENDICULAR TO THE LOS AND AT THE SOURCE DISTANCE
FROM THE OBSERVER ) IN THE USER COORDINATE SYSTEM.
POINT SPACING IS    0.125 M       UNITS: Watts/m**2/sr/um
```

Figure 11. Apparent temperature plots for various wind directions. Prepared from the data files of the example 9 simulation. Wavelength was 3.6 μm.

References

Beyer, W. H., ed., *CRC Standard Mathematical Tables*, 26 ed., CRC Press Inc., Boca Raton, FL, 1981.

Briggs, G. A., *Plume Rise*, U.S. Atomic Energy Commission, TID-25075, Oak Ridge, TN, 1969.

Bruce, C. W., and N. M. Richardson, "Propagation at 10 μm Through Smoke Produced by Atmospheric Combustion of Diesel Fuel," *Applied Optics*, 22(7):1051-1055, 1983.

Bruce, C. W., S. B. Crow, Y. P. Yee, B. D. Hinds, D. Marlin, and A. V. Jelinek, "Infra-Red Optical Properties of Diesel Smoke Plumes," *Applied Optics*, 28(19):4071-4076, 1989.

Bruce, C. W., T. F. Stromberg, K. P. Gurton, and J. B. Mozer, "Trans-Spectral Absorption and Scattering of Electromagnetic Radiation by Diesel Soot," *Applied Optics*, 30(12):1537-1546, 1991.

Bruce, D., *Fire-Induced Transmission and Turbulence Effects Module FITTE*, ASL-TR-0221-15, US Army Atmospheric Sciences Laboratory, White Sands Missile Range, NM 88002-5501, 1987.

Bruce, D., "An Extended Emissive Source Simulation Model," In *Proceedings of the Society of Photo-Optical Instrumentation Engineers*, Vol 926, SPIE, Bellingham, WA 98227-0010, 1988.

Bruce, D., "A Comparison of Modelled Thermal Images of Fires with Field Test Data," In *Proceedings of the Smoke/Obscurants Symposium XIII*, AMCPM-SMK-CT-001-89, OPM Smoke/Obscurants, Aberdeen Proving Ground, MD 21005, 1989.

Bruce, D., and R. A. Sutherland, "FITTE Model Validation: A Status Report," In *Proceedings of the Sixth Annual EOSAEL/TWI Conference*, US Army Atmospheric Sciences Laboratory, White Sands Missile Range, NM 88002-5501, 1986.

Bruce, D., R. A. Sutherland, and D. Larson, "Fire-Induced Transmission and Turbulence Effects Module FITTE," *EOSAEL 82: Vol III, Transmission Through Battlefield Aerosols*, ASL-TR-0122, US Army Atmospheric Sciences Laboratory, White Sands Missile Range, NM 88002-5501, 1982.

Chylek, P., V. Ramaswamy, R. Cheng, and R. G. Pinnick, "Optical Properties and Mass Concentrations of Carbonaceous Smokes," *Appl. Opt.*, **20**, p 2980-2985, 1981.

Fante, R. L., "Electromagnetic Beam Propagation in Turbulent Media," In *Proceedings IEEE*, 63(12):1669-1692, 1975.

Farmer, W. M., B. Locke, R. E. Davis, and R. Laughman, *U.S. Army Transmissometer Validation Program-Summary Report*, STC Technical Report 3003, Science and Technology Corporation, 555 S. Telshor Blvd., Las Cruces, NM 88005, 1989.

George, W. K., R. L. Alpert, and F. Tamanini, "Turbulence Measurements in an Axisymmetric Buoyant Plume," *Int J Heat Mass Transfer*, 20:1145-1154, 1977.

Gillespie, P. S., *BEST-ONE Data Analysis and Comparison*, OMI-237, OptiMetrics, Inc., 106 E. Idaho, Suite G, Las Cruces, NM 88005, 1987.

Gomez, R. B., R. A. Sutherland, L. S. Levitt, and E. A. Olivas, "Products of Vehicle and Grass Fires Affecting Electro-Optical System Performance," In *Proceedings of the Society of Photo-Optical Instrumentation Engineers*, Vol 219, Los Angeles Technical Symposium, 1980.

Hoult, D. P., J. A. Fay, and L. J. Forney, "A Theory of Plume Rise Compared with Field Observations," *J. Air Pollut. Control Ass.*, 19:585-590, 1969.

Hoult, D. P., and J. C. Weil, "A Turbulent Plume in a Laminar Crossflow," *Atmos. Environ.*, 6:513-531, 1972.

Kaaijk, J., *Chemical Characterization of Fire Products*, PML 1986-47, Prins Maurits Laboratorium, P.O. Box 45, 2280 AA rijswijk, The Netherlands, 1986.

Kennedy, B. W., *Battlefield Induced Contamination Test Project Summary*, Internal Report, U.S. Army Atmospheric Sciences Laboratory, White Sands Missile Range, NM, 1981.

Kennedy, B. W., *Battlefield Induced Contamination Test-III (BICT III)*, Internal Report, U.S. Army Atmospheric Sciences Laboratory, White Sands Missile Range, NM, 1982.

Khanna, R., E. Burlbaw, and A. Deepak, *Models for Macrophysical and Microphysical Properties of Fire Products*, Final Report, Contract DAAG29-81-D-0100, U.S. Army Atmospheric Sciences Laboratory, White Sands Missile Range, NM, 1982.

Khanna, R. K., and H. L. Ammon, *Optical Properties of Vehicular and Vegetative Fire Products*, Technical Report 525, DAA629-81-D-0100, Battelle Columbus Laboratories, Columbus, OH, 1983.

Kneizys, F. X., E. P. Shettle, W. O. Gallery, J. H. Chetwynd, Jr., L. W. Abreu, J. E. A. Selby, S. A. Clough, and R. W. Fenn, *Atmospheric Transmittance/Radiance: Computer Code LOWTRAN 6*, AFGL-TR-83-0187, Air Force Geophysics Laboratory, Hanscom AFB, Bedford, MA, 1983.

Liedner, L., and D. Clement, "Radiation Properties of Fires Derived from BEST ONE Data," In *Proceedings of the Workshop on Measuring and Modelling the Battlefield Environment*, North Atlantic Treaty Organization, Brussels, Belgium, 337-346, 1987.

Leslie, D. H., P. G. Eitner, J. L. Manning, and S. M. Singer, *Infrared Electro-Optical System Performance Effects Due to Absorption by Battlefield Gases*, ASL-CR-80-0127-2, U.S. Army Atmospheric Sciences Laboratory, White Sands Missile Range, NM, 1980.

Levitt, B. W., and L. S. Levitt, "Identification and Assessment of Factors Important in Modeling of Electro-Optical System Performance in Realistic Fire Situations," *Optical Engineering*, 21:148, 1982.

Manning, J. L., *Addition of Molecular Transmittance and Radiance to Computer Code FITTE*, OMI-136, OptiMetrics, Inc., 2000 Hogback Rd., Suite 3, Ann Arbor, MI, 1985.

Manning, J. L., and K. A. Kebschull, *The FfO 88 Version of the FITTE Code*, OMI-292, OptiMetrics, Inc., 2008 Hogback Road, Suite 6, Ann Arbor, MI, 1988.

Pinnick, R. G., G. Fernandez, B. D. Hinds, and P. Fishburn, *Vehicular Dust and Fire Products Particle Size and Concentration Measurements in BIC-1 and BIC-2*, Internal Report, U.S. Atmospheric Sciences Laboratory, White Sands Missile Range, NM, unpublished data, 1982.

Strohbehn, J. W., editor, "Laser Beam Propagation in the Atmosphere," *Topics in Applied Physics*, **25**, Springer-Verlag, 1978.

Sutherland, R. A., and P. L. Walker, "Modelling Fire Products," In *Proceedings of Smoke Symposium VI*, DRCPM-SMK-T-001-82, Harry Diamond Laboratories, Adelphi, MD, 1982.

Tatarski, V. I., *The Effects of the Turbulent Atmosphere on Wave Propagation*, U.S. Department of Commerce, Washington, DC, 1971.

Thompson, J. H., and J. G. DeVore, *Analysis and Modelling of Battlefield Fire Plumes*, ASL-CR-81-0072-2, U.S. Army Atmospheric Sciences Laboratory, White Sands Missile Range, NM, 1981.

Turner, R. E., P. G. Eitner, and J. L. Manning, *Analysis of Battlefield-Induced Contaminants for E-O SAEL*, ASL-CR-80-0032, U.S. Army Atmospheric Sciences Laboratory, White Sands Missile Range, NM, 1980.

Weil, J. C., "Source Buoyancy Effects in Boundary Layer Diffusion," In *Proceedings of the Workshop on the Parameterization of Mixed Layer Diffusion*, Physical Sciences Laboratory, New Mexico State University, Las Cruces, NM, 1981.

Wyngaard, J. C., "On Surface Layer Turbulence," *Workshop on Micrometeorology*, D. A. Haugen, editor, Amer. Meteor. Soc., Boston, MA, 1973.

Young, S. J., *Description and Use of the Plume Radiation Code ATLES*, SAMSO-TR-77-100, Aerospace Corporation, El Segundo, CA, 1977.

Acronyms and Abbreviations

ARL	Army Research Laboratory
ASL	Atmospheric Sciences Laboratory
BEST ONE	Battlefield Emissive Sources Trial, Oldebruck, the Netherlands, Europe
BICT I	Battlefield Induced Contamination Test I
BICT III	Battlefield Induced Contamination Test III
EOSAEL	Electro-Optical Systems Atmospheric Effects Library
FITTE	Fire-Induced Transmittance and Turbulence Effects
IR	infrared
LOS	line of sight

Appendix A

Fluctuation Time-History Data Files

A-1. Basic Ideas Underlying the Fluctuation Data Files

Fire plumes move about in space as a function of time. The fluctuations of the centerline position at a given plume height are a result of fluctuations in the horizontal windspeed and wind direction since that plume segment was generated. The centerline fluctuations can be described by a deterministic model if the wind fluctuations are known. The fluctuations in temperature and effluent concentrations at any point in the plume are the result of turbulent mixing. For a simple fast-running model, the fluctuations can be approximated by a distribution with a turbulent power spectral density with amplitudes and phase angles based on random numbers. The amplitude fluctuations can be scaled using available data.

The minimum information needed to model a space- and time-varying (4D) plume is a set of random numbers and x- and y-wind fluctuation data.

Several additional considerations related to model simplicity were used in constructing the files:

• A 1-s time step was defined for the calculations. The row number in the file corresponds to the number of seconds after the start of the fire. The data file must be long enough to describe plume transport after the fire burns out, so a total file length of 2000 rows was chosen.

• It is desirable to be able to use the fluctuation data files for a range of windspeeds, so the wind fluctuation data should be normalized; the data stored should be fractional fluctuations.

• Calculations of centerline displacement are based on the cumulative fluctuations since the displaced plume segment was created. These calculations are most easily and quickly performed if the wind fluctuation data are stored as cumulative fractional fluctuations.

If model performance is to be compared with data from field tests, it is desirable to use a time-history file that reflects the wind conditions during the test. Construction of such a file is described below.

A-2. Construction of a Time-History File from Field Test Data

A time-history file may be constructed from field test data if data meet the following criteria:

- include windspeed and wind direction
- available at 1-s intervals
- contain (at least) 2000 observations.

The 2000 s of data must be averaged to obtain mean windspeed and wind direction. The mean windspeed and wind direction should be recorded for use as input on the METD input card. The data must be processed to obtain time-histories of windspeed in and perpendicular to the mean wind direction.

The data can be transformed and stored in a time-history file. The file, as mentioned earlier in the manual, must have three columns of data. The first column must contain a set of random numbers in the range -0.5 to 0.5, and a mean of 0.00 ± 0.009. The second column must contain the cumulative normalized fluctuations in the downwind component of the wind. If we define the mean windspeed as U and the instantaneous windspeed in the mean wind direction as u_i, the value in the nth row of the second column is given by

$$\frac{1}{U} \sum_{1}^{n} (u_i - U). \qquad \text{(A-1)}$$

The third column of the data file contains the cumulative normalized crosswind component. If we define the instantaneous value of the crosswind component to be v_i, the value in the nth row of the third column is given by

$$\frac{1}{U} \sum_{1}^{n} v_i . \qquad \text{(A-2)}$$

The time-history file is read with an unformatted READ statement that requires three values for each row, so the columnar values for each row should be separated by spaces or other separators recognized by FORTRAN.

93

You should rename the existing file FIT4D.DAT and copy the desired time-history file into FIT4D.DAT, because it is the filename used by FITTE for the time-history file.

Appendix B

Auxiliary Programs for Visualization of FGLOW Output

Two accessory programs are provided to help with visualization of the image files created by FITTE. The accessory programs are working examples that transform the FGLOWn.FDT files into forms that may be printed or imported into a graphics program that can produce contour plots. Both of the programs permit output of four quantities: radiance, transmittance, apparent (blackbody-equivalent) temperature, and integrated path density (CL). The latter two quantities are obtained by transformation of the first two for the appropriate wavelength. (This would be the central wavelength for a waveband calculation.)

SEPARATE SIMULATION RUNS ARE NO LONGER NECESSARY TO OBTAIN APPARENT TEMPERATURE IMAGES.

The FGLOWn.FDT output files, generally, should be renamed for storage; otherwise, they will be overwritten the next time FITTE is run using the FGLOW identifier.

The programs are written for use with equipment and software that we have on hand. This should not be construed as a recommendation or endorsement of the hardware and software.

Plots prepared with output from XS2GRD were shown in section 5 with sample runs. Appendix B contains a sample of output from XS2PRT.

B-1. XS2PRT

XS2PRT creates files containing greyscale printouts of the FGLOWn.FDT data. The files have the same name as the input file with the extension FDT replaced by RAD, TRN, APT, or DNS as appropriate. The example program is tailored for an HP Laserjet printer and uses control sequences and built-in fonts in creating the output files. The width of the image array (that is, the number of columns in the array) determines whether the output is printed in portrait or landscape mode or is split into panels for printing.

If another printer is used for the printouts, it is necessary to modify the program. This entails substitution of the appropriate printer control sequences

(usually found in the printer manual) and modification of the numbers that determine when to split the output into panels. Fixed spacing fonts should be used, and the number of characters per inch should be (nearly) equal to the number of lines per inch to give the image the correct proportions. The program is relatively well commented to assist in identifying areas needing changes.

Figure B-1 shows a printout of integrated path density created using this program. The simulation file was the same file used to create the plume transmittance contour image shown in figure 4. The greyscale assignment table was moved to the same page as the image for this example.

B-2. XS2GRD

XS2GRD transforms the FGLOWn.FDT files to a form that commercial software uses to create surface or contour plots. This program should be relatively easy to modify for use with other plotting packages. The format for the output file is described in program comments.

Because the program used for the contour plots expects a file extension of .GRD, the output files for this program have the extension .FDT replaced by R.GRD, T.GRD, A.GRD, or D.GRD depending on which of the four types of data it contains.

SIMULATION FILE IS C:\FIG3M.FDT : PLUME DENSITY (CL)   FOR WAVELENGTH
    0.630000   uM, IMAGE WIDTH, HEIGHT (M):   60.0000   ,   40.0000
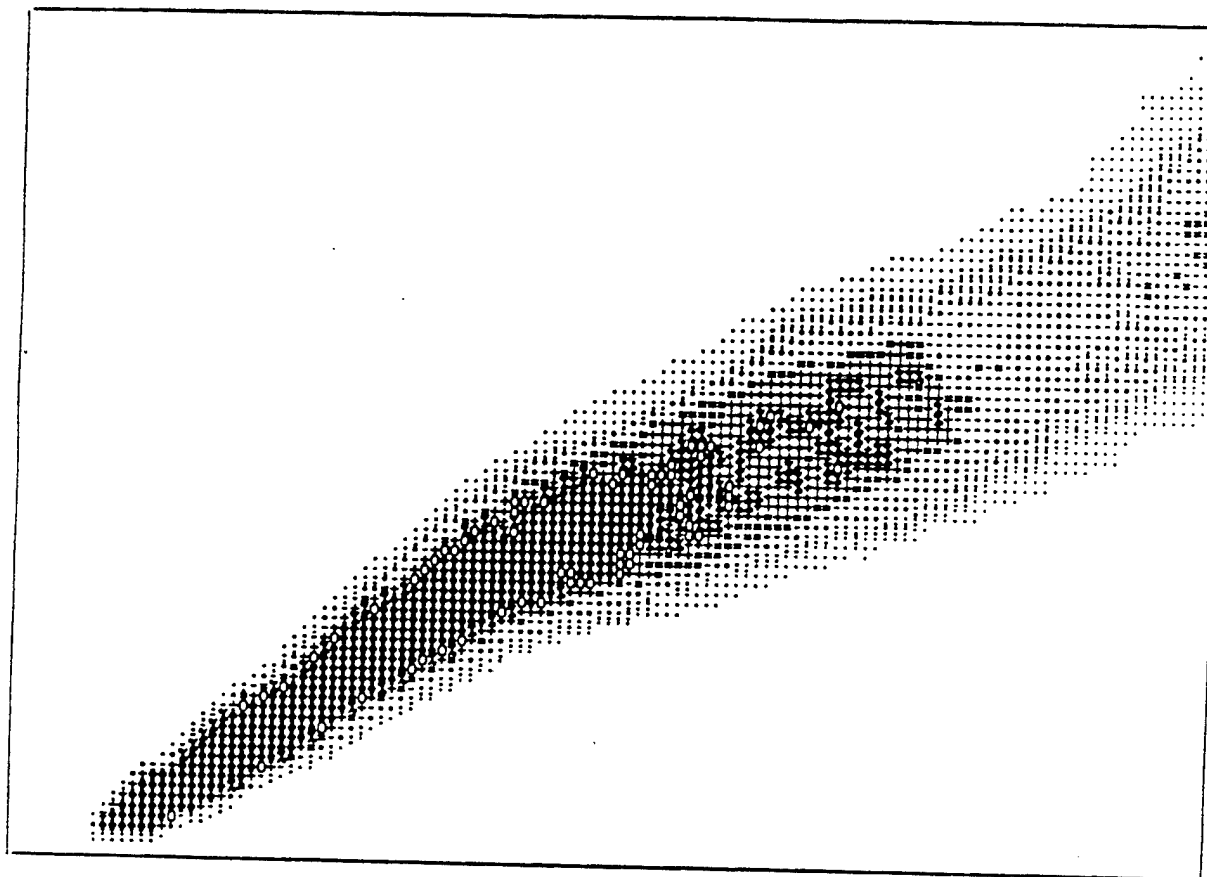
KEY TO IMAGE VALUES:

	FROM	0.000000	TO	0.557446E-01
.	FROM	0.557446E-01	TO	0.111489
:	FROM	0.111489	TO	0.167234
•	FROM	0.167234	TO	0.222978
−	FROM	0.222978	TO	0.278723
=	FROM	0.278723	TO	0.334468
÷	FROM	0.334468	TO	0.390212
+	FROM	0.390212	TO	0.445957
%	FROM	0.445957	TO	0.501701
o	FROM	0.501701	TO	0.557446
Φ	FROM	0.557446	TO	0.613190
θ	FROM	0.613190	TO	0.668935
≡	FROM	0.668935	TO	0.724680
	FROM	0.724680	TO	0.780424
	FROM	0.780424	TO	0.836169
	FROM	0.836169	TO	0.891913

Figure B-1. Greyscale print of plume optical density produced with XS2PRT.

98

Appendix C

Modification of Fire Parameters

The selection of fire parameters to provide realistic representations within the model is not a simple, straightforward process. There are also limitations, primarily imposed by model assumptions that limit the fires that can be described. Appendix C discusses the limitations, describes rough relations between model and physical fire parameters, and suggests limits on parameter variation using the SVAR input card.

C-1. Model Limitations on Fire Parameters

FITTE was developed as a fast running code to model effects of small-scale battlefield fires that were assumed to be vehicular fires. Table C-1 shows basic assumptions made (consistent with this objective) and associated model limitations. The first and second assumptions must be considered when fire parameters are varied. The size limits shown are approximate. It is difficult to set bounds for the heat output, but the values associated with the fires defined in the model are the right order of magnitude.

Table C-1. Limitations caused by model assumptions

Model Assumption	Associated Limitations
1. The energy density of the fire plume is low compared with that of the atmosphere.	Only small-scale fires ($R < 10$ m) with low to moderate heat output can be handled.
2. The plume must have structural integrity.	The fire has a minimum size ($R \geq 0.5$ m) and heat flux.
3. The mean plume centerline is described by a power law.	Unusual wind-shear conditions cannot be handled. Less accuracy under very low windspeed conditions.
4. Fires are assumed to be circular.	Cannot easily be adapted to describe linear fires, such as grass fires.

The limits are intended to indicate that model predictions have built-in unknown errors if parameters are varied to describe other fires, like an oil well fire because it is a high-energy density source.

The parameters that can be varied using the input card SVAR are mean fire temperature, aerosol efficiency factor, fire radius, and burn time. It is possible to vary these parameters to examine the effect of uncertainties associated with their values or to provide a better comparison with field test data.

Variation of the parameters to examine the effect of uncertainties associated with their values was discussed briefly in section 4. For providing a better comparison with field test data, the following comments may be useful.

C-1.1 *Developing Model Fire Parameters from Data*

The burn time can be obtained from observations. The associated uncertainty lies in determining the end time for the fire. The end time should be chosen as the time when a cohesive plume ceases to exist.

The fire radius has a clear meaning for a pool fire in a circular tank. If another container shape is involved, such as a rectangular tank of dimensions L by W with L < 2W, an appropriate value would probably be R = 0.5 (L + W). The exact shape is not critical because the influx of air modifies the shape of the fire or fire plume so it is quasicircular.

The mean fire temperature can be estimated from a set of measurements above the fire. This can be tricky for a fire in the field, and the estimate will have a relatively large uncertainty. The value used in the model was obtained as follows (using Kelvin temperatures):

1. The data were examined to obtain the (average of the) maximum observed temperatures for the thermocouples near the center of the fire. (The thermocouple array was at about the level of the flame tips.) The (average) value was assumed to be valid for a point at a radius of 1σ from the center of

a Gaussian distribution. (The wind shifted the fire about, and the thermocouple array was in an area with a narrow distribution function.)

2. The value was divided by exponent(-.5) to obtain an estimate of the Gaussian maximum.

3. The ambient temperature was subtracted from the Gaussian maximum temperature to obtain the excess plume maximum temperature. The excess plume maximum temperature was divided by 2.9; the ratio of Gaussian/top hat distribution values for the observation conditions. The ambient temperature was then added to obtain the mean fire temperature.

It is extremely difficult to obtain a good measurement of the aerosol efficiency factor. The value built into FITTE should be appropriate under most conditions.

C-1.2   Checking Model Behavior When Varying Fire Parameters

If plume image data (photographs, video, or infrared images) are available, it is possible to check the plume behavior to ensure that the fire parameters produce a realistic plume. The following checks may be made by comparing the data with information derived from the model output. The most accurate checks are based on images taken from a crosswind position.

The quantities to be checked are the initial plume slope and spread. A scenario 1 model run with the fire parameter variation produces output that may be used to predict these values.

The ratio of the vertical wind to the windspeed gives the initial plume slope. The inverse tangent predicts the initial elevation angle. The elevation angle should be compared with the slope or elevation angle obtained from the plume images. A short segment of the plume image should give the best value for the angle. (You may want to try this comparison with example 10 to get an idea of the errors involved.)

The plume spread angle is the inverse tangent of the entrainment constant. You should compare the plume spread angle with the (full width) angular spread of the plume obtained from the images. Use as long a plume segment as possible for the most accurate result.

If agreement is good for both comparisons, the model should provide good predictions of the propagation effects when the selected fire parameters are used. Good agreement for the initial elevation angle depends on the variability of the wind during the field test as well as the uncertainty in determining the angle from the images. The plume spread angle should agree within 5°.

A scenario 3 run could also be used; a printed simulated image could be produced with the accessory program XS2PRT and could be compared directly with the real plume images.

Appendix D

Model Organization

Figure D-1 shows the organization of FITTE. It can be called from EOSAEL main, or run as a stand-alone driver called by FITDRV.FOR. If FITDRV.FOR is used, it and its corresponding block data subroutine BLOCD.FOR must be customized for the system on which it is to be run.

In general, the subroutines called directly by FITTE are called once, except for XSMIT which is called once for each path segment. For scenario 3, SETLOS is called to establish parameter values for each line of sight (LOS) of the image matrix.

The FITTE model consists of 26 subroutines and 12 functions. EOSAEL main or FITDRV.FOR is used as the main program, and the corresponding block data routines, FITTBD and BLOCD, respectively, must be linked with the program.

A brief description of each subroutine and function is given below. The subroutines are listed roughly as they are first called. Subroutines that perform specific related calculations are grouped together.

D-1. Subroutines

D-1.1 **FITTE**

FITTE is the subroutine that controls execution of the model. It calls subroutines to perform required calculations and write model output files.

D-1.2 **FITTRD**

FITTRD controls reading of the FITTE input cards, checks the input values, substitutes defaults if possible when invalid data are encountered, and calls subroutines to transform coordinates and units and calculate plume constants for given input parameters.

D-1.2.1   *XSFORM.*—XSFORM transforms EOSAEL common block input to units used by FITTE.
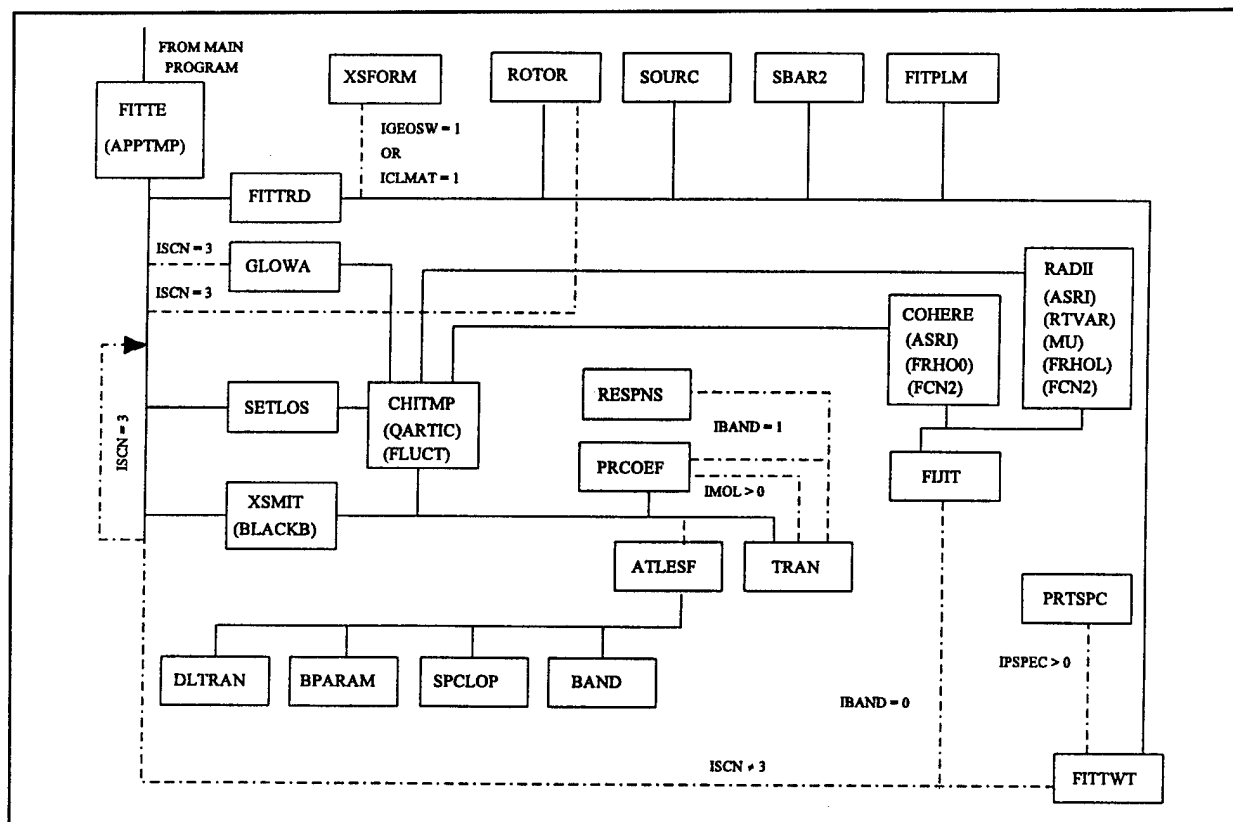
Figure D-1. Diagram of FITTE model structure. Dashed lines indicate conditional calls. Functions called, except EXPOF, are listed in parentheses in subroutine boxes.

D-1.2.2   *ROTOR.*—ROTOR transforms coordinates to (and from) the wind-aligned system used by FITTE.

D-1.2.3   *SOURC.*—SOURC sets values of fire parameters based on input from the REFD card and the SVAR card. Table 1 of this document shows the parameters for the various sources.

D-1.2.4   *SBAR2.*—SBAR2 calculates the stability parameter needed to calculate the ambient lapse rate for FITTE. The routine is identical with subroutine SBAR1 used in the EOSAEL 82 version of model COMBIC.

D-1.2.5   *FITPLM.*—FITPLM calculates the values of FITTE plume parameters.

107

D-1.3 GLOWA

GLOWA is called to calculate parameters needed for control of FGLOW (ISCN = 3) model execution.

D-1.4 CHITMP

CHITMP calculates values of plume distribution functions, such as temperature and aerosol and molecular densities for a given point on the LOS.

D-1.4.1 FLUCT1.—FLUCT1 calculates the displacement, caused by wind fluctuations, of a plume centerline point from the mean centerline for the current calculation time.

D-1.4.2 FLUCT2.—FLUCT2 calculates fluctuations in entrainment and combustion products caused by wind fluctuations.

D-1.5 SETLOS

SETLOS calculates plume entry and exit points on the LOS.

D-1.6 XSMIT

XSMIT controls calculation of the propagation parameters related to extinction and radiance. When molecular absorption effects are to be included (IMOL <> 0), it calls the set of subroutines adapted from the ATLES model code.

D-1.7 ATLESF

ATLESF controls calculations of molecular absorption by the combustion products carbon dioxide and water vapor. Temperature-dependent absorption coefficients are used for the calculations. Values are calculated for each of the NWVN wavenumbers if a waveband calculation is specified.

D-1.7.1 BAND.—BAND reads the temperature-dependent band model parameters.

108

D-1.7.2   *SPCLOP.*—SPCLOP creates an array IWAVE to control the band model calculations.

D-1.7.3   *BPARAM.*—BPARAM calculates band model parameters for a given wave number, path segment, and species of molecule.

D-1.7.4   *DLTRAN.*—DLTRAN calculates the transmittance along a path segment for a single molecular species.

D-1.8   TRAN

TRAN averages transmittances and integrates radiances over the waveband. It calls RESPNS to create an instrument response function array for use in these calculations, and it calls PRCOEF to obtain the aerosol optical constants for each wavelength. For single wavelength calculations, it transfers values from the calculation arrays to the output variables.

D-1.9   RESPNS

RESPNS calculates an array of instrument response coefficients for the wave numbers used in a waveband calculation.

D-1.10   PRCOEF

PRCOEF assigns values of aerosol optical constants for a given wavelength.

D-1.11   FIJIT

FIJIT controls calculation of the optical turbulence effects parameters. It calls one or both of the routines listed below, depending on the FITTE scenario specified.

D-1.11.1   *COHERE.*—COHERE calculates the lateral coherence length by using function ASRI to integrate the function FRHOO through the plume.

D-1.11.2 RADII.—RADII performs the calculations described by Fante (1975), using ASRI to perform the necessary integrations. It assigns a value to ICASE to indicate which of the four calculation methods was used.

D-1.12 *FITTWT*

FITTWT controls formatting and printing of user input and model output. The output is tailored to the specified scenario. A warning is printed if defaults were substituted for any of the user-specified variables, and an error message is printed if fatal input data are detected. The value of MODE is used to specify whether input or output is written.

D-1.12.1 PRTSPC.—PRTSPC prints a table of spectrally resolved transmittance and radiance data.

D-2. Functions

D-2.1 *APPTMP*

APPTMP is an inverse blackbody function used to produce apparent temperature output for FGLOW if IAPT = 1. For a waveband calculation, the evaluation is performed for the wavelength at the center of the band.

D-2.2 *ASRI*

ASRI is an adaptive Simpson's rule integration routine with a specified local error and a maximum permitted number of resolution increases. If the function being integrated does not meet the error tolerance after the maximum number of resolutions increases for a given path interval, a flag is set to indicate that the integration error is greater than that specified.

D-2.3 *BLACKB*

BLACKB calculates the energy density of a blackbody of temperature T at wavelength λ.

D-2.4 EXPOF

EXPOF limits the allowed range of exponents to prevent program crashes caused by calculation errors.

D-2.5 FCN2

FCN2 evaluates C_n^2 as a function of temperature at any point in the plume.

D-2.6 FLUCT3

FLUCT3 evaluates the local fractional fluctuation in plume temperature based on the assumption of a fractal spatial frequency distribution.

D-2.7 FLUCT4

FLUCT4 evaluates the local fractional fluctuation in plume effluents based on the assumption of a fractal spatial frequency distribution.

D-2.8 FRHO0

FRHO0 evaluates the integrand in the equation for RHO0 in subroutine COHER.

D-2.9 FRHOL

FRHOL evaluates the integrand in the equation for ρ_L in subroutine RADII.

D-2.10 MU

MU evaluates the ratio of short- to long-term averaged beam radius using numerical results (Fante 1975). This function is used by subroutine RADII for case 2 calculations as described in the technical manual.

D-2.11 *QARTIC*

QARTIC solves a quartic equation to find the centerline point closest to a given LOS point. It is called by CHITMP.

D-2.12 *RTVAR*

RTVAR evaluates the variance of 1/T for function FCN2 of subroutine RADII. It uses a look-up table and an interpolation scheme.

Distribution

Copies

ARMY CHEMICAL SCHOOL   1
ATZN CM CC
ATTN MR BARNES
FT MCCLELLAN AL 36205-5020

NASA MARSHAL SPACE FLT CTR   1
ATMOSPHERIC SCIENCES DIV
E501
ATTN DR FICHTL
HUNTSVILLE AL 35802

NASA SPACE FLT CTR   1
ATMOSPHERIC SCIENCES DIV
CODE ED 41 1
HUNTSVILLE AL 35812

ARMY STRAT DEFNS CMND   1
CSSD SL L
ATTN DR LILLY
PO BOX 1500
HUNTSVILLE AL 35807-3801

ARMY MISSILE CMND   1
AMSMI RD AC AD
ATTN DR PETERSON
REDSTONE ARSENAL
AL 35898-5242

ARMY MISSILE CMND   1
AMSMI RD AS SS
ATTN MR H F ANDERSON
REDSTONE ARSENAL
AL 35898-5253

ARMY MISSILE CMND   1
AMSMI RD AS SS
ATTN MR B WILLIAMS
REDSTONE ARSENAL
AL 35898-5253

ARMY MISSILE CMND   1
AMSMI RD DE SE
ATTN MR GORDON LILL JR
REDSTONE ARSENAL
AL 35898-5245

ARMY MISSILE CMND   1
REDSTONE SCI INFO CTR
AMSMI RD CS R DOC
REDSTONE ARSENAL
AL 35898-5241

ARMY MISSILE CMND   1
AMSMI
REDSTONE ARSENAL
AL 35898-5253

ARMY INTEL CTR   1
AND FT HUACHUCA
ATSI CDC C
FT HUACHUCA AZ 85613-7000

NAVAL WEAPONS CTR   1
CODE 3331
ATTN DR SHLANTA
CHINA LAKE CA 93555

PACIFIC MISSILE TEST CTR   1
GEOPHYSICS DIV
ATTN CODE 3250
POINT MUGU CA 93042-5000

LOCKHEED MIS & SPACE CO   1
ATTN KENNETH R HARDY
ORG 91 01 B 255
3251 HANOVER STREET
PALO ALTO CA 94304-1191

NAVAL OCEAN SYST CTR   1
CODE 54
ATTN DR RICHTER
SAN DIEGO CA 92152-5000

METEOROLOGIST IN CHARGE   1
KWAJALEIN MISSILE RANGE
PO BOX 67
APO SAN FRANCISCO
CA 96555

DEPT OF COMMERCE CTR   1
MOUNTAIN ADMINISTRATION
SPPRT CTR LIBRARY R 51
325 S BROADWAY
BOULDER CO 80303

DR HANS J LIEBE   1
NTIA ITS S 3
325 S BROADWAY
BOULDER CO 80303

NCAR LIBRARY SERIALS   1
NATL CTR FOR ATMOS RSCH
PO BOX 3000
BOULDER CO 80307-3000

DEPT OF COMMERCE CTR   1
325 S BROADWAY
BOULDER CO 80303

DAMI POI   1
WASH DC 20310-1067

MIL ASST FOR ENV SCI OFC   1
OF THE UNDERSEC OF DEFNS
FOR RSCH & ENGR R&AT E LS
PENTAGON ROOM 3D129
WASH DC 20301-3080

DEAN RMD   1
ATTN DR GOMEZ
WASH DC 20314

ARMY INFANTRY   1
ATSH CD CS OR
ATTN DR E DUTOIT
FT BENNING GA 30905-5090

AIR WEATHER SERVICE   1
TECH LIBRARY FL4414 3
SCOTT AFB IL 62225-5458

USAFETAC DNE   1
ATTN MR GLAUBER
SCOTT AFB IL 62225-5008

HQ AWS DOO 1   1
SCOTT AFB IL 62225-5008

ARMY SPACE INSTITUTE   1
ATTN ATZI SI 3
FT LEAVENWORTH
KS 66027-5300

PHILLIPS LABORATORY   1
PL LYP
ATTN MR CHISHOLM
HANSCOM AFB MA 01731-5000

ATMOSPHERIC SCI DIV   1
GEOPHYSICS DIRCTRT
PHILLIPS LABORATORY
HANSCOM AFB MA 01731-5000

PHILLIPS LABORATORY   1
PL LYP 3
HANSCOM AFB MA 01731-5000

RAYTHEON COMPANY   1
ATTN DR SONNENSCHEIN
528 BOSTON POST ROAD
SUDBURY MA 01776
MAIL STOP 1K9

ARMY MATERIEL SYST   1
ANALYSIS ACTIVITY
AMXSY
ATTN MP H COHEN
APG MD 21005-5071

ARMY MATERIEL SYST   1
ANALYSIS ACTIVITY
AMXSY AT
ATTN MR CAMPBELL
APG MD 21005-5071

ARMY MATERIEL SYST   1
ANALYSIS ACTIVITY
AMXSY CR
ATTN MR MARCHET
APG MD 21005-5071

ARL CHEMICAL BIOLOGY   1
NUC EFFECTS DIV
AMSRL SL CO
APG MD 21010-5423

ARMY MATERIEL SYST   1
ANALYSIS ACTIVITY
AMXSY
APG MD 21005-5071

NAVAL RESEARCH LABORATORY   1
CODE 4110
ATTN MR RUHNKE
WASH DC 20375-5000

ARMY MATERIEL SYST   1
ANALYSIS ACTIVITY
AMXSY CS
ATTN MR BRADLEY
APG MD 21005-5071

ARMY RESEARCH LABORATORY   1
AMSRL D
2800 POWDER MILL ROAD
ADELPHI MD 20783-1145

ARMY RESEARCH LABORATORY   1
AMSRL OP SD TP
TECHNICAL PUBLISHING
2800 POWDER MILL ROAD
ADELPHI MD 20783-1145

ARMY RESEARCH LABORATORY   1
AMSRL OP CI SD TL
2800 POWDER MILL ROAD
ADELPHI MD 20783-1145

ARMY RESEARCH LABORATORY   1
AMSRL SS SH
ATTN DR SZTANKAY
2800 POWDER MILL ROAD
ADELPHI MD 20783-1145

ARMY RESEARCH LABORATORY   1
AMSRL
2800 POWDER MILL ROAD
ADELPHI MD 20783-1145

118

NATIONAL SECURITY AGCY W21   1
ATTN DR LONGBOTHUM
9800 SAVAGE ROAD
FT GEORGE G MEADE
MD 20755-6000

OIC NAVSWC   1
TECH LIBRARY CODE E 232
SILVER SPRINGS
MD 20903-5000

ARMY RESEARCH OFFICE   1
AMXRO GS
ATTN DR W BACH
PO BOX 12211
RTP NC 27709

DR JERRY DAVIS   1
NCSU
PO BOX 8208
RALEIGH NC 27650-8208

ARMY CCREL   1
CECRL GP
ATTN DR DETSCH
HANOVER NH 03755-1290

ARMY ARDEC   1
SMCAR IMI I BLDG 59
DOVER NJ 07806-5000

ARMY COMMUNICATION   1
ELECTR CTR FOR EW RSTA
AMSEL RD EW SP
FT MONMOUTH NJ 07703-5206

ARMY SATELLITE COMM AGCY   1
DRCPM SC 3
FT MONMOUTH NJ 07703-5303

ARMY COMMUNICATIONS   1
ELECTR CTR FOR EW RSTA
AMSEL EW D
FT MONMOUTH NJ 07703-5303

ARMY COMMUNICATIONS   1
ELECTR CTR FOR EW RSTA
AMSEL EW MD
FT MONMOUTH NJ 07703-5303

ARMY DUGWAY PROVING GRD   1
STEDP MT DA L 3
DUGWAY UT 84022-5000

ARMY DUGWAY PROVING GRD   1
STEDP MT M
ATTN MR BOWERS
DUGWAY UT 84022-5000

DEPT OF THE AIR FORCE   1
OL A 2D WEATHER SQUAD MAC
HOLLOMAN AFB
NM 88330-5000

PL WE   1
KIRTLAND AFB NM
87118-6008

USAF ROME LAB TECH   1
CORRIDOR W STE 262 RL SUL
26 ELECTR PKWY BLD 106
GRIFFISS AFB
NY 13441-4514

AFMC DOW   1
WRIGHT PATTERSON AFB
OH 0334-5000

ARMY FIELD ARTLLRY SCHOOL   1
ATSF TSM TA
FT SILL OK 73503-5600

120

NAVAL AIR DEV CTR   1
CODE 5012
ATTN AL SALIK
WARMINISTER PA 18974

ARMY FOREGN SCI TECH CTR   1
CM
220 7TH STREET NE
CHARLOTTESVILLE
VA 22901-5396

NAVAL SURFACE WEAPONS CTR   1
CODE G63
DAHLGREN VA 22448-5000

ARMY OEC   1
CSTE EFS
PARK CENTER IV
4501 FORD AVE
ALEXANDRIA VA 22302-1458

ARMY CORPS OF ENGRS   1
ENGR TOPOGRAPHICS LAB
ETL GS LB
FT BELVOIR VA 22060

TAC DOWP   1
LANGLEY AFB
VA 23665-5524

ARMY TOPO ENGR CTR   1
CETEC ZC 1
FT BELVOIR VA 22060-5546

LOGISTICS CTR   1
ATCL CE
FT LEE VA 23801-6000

SCI AND TECHNOLOGY   1
101 RESEARCH DRIVE
HAMPTON VA 23666-1340

ARMY NUCLEAR CML AGCY   1
MONA ZB BLDG 2073
SPRINGFIELD VA 22150-3198

ARMY FIELD ARTLLRY SCHOOL   1
ATSF F FD
FT SILL OK 73503-5600

USATRADOC   1
ATCD FA
FT MONROE VA 23651-5170

ARMY TRADOC ANALYSIS CTR   1
ATRC WSS R
WSMR NM 88002-5502

ARMY RESEARCH LABORATORY   1
AMSRL BE M
BATTLEFIELD ENVIR DIR
WSMR NM 88002-5501

ARMY RESEARCH LABORATORY   1
AMSRL BE A
BATTLEFIELD ENVIR DIR
WSMR NM 88002-5501

ARMY RESEARCH LABORATORY   1
AMSRL BE W
BATTLEFIELD ENVIR DIR
WSMR NM 88002-5501

ARMY RESEARCH LABORATORY   1
AMSRL BE
ATTN MR VEAZEY
BATTLEFIELD ENVIR DIR
WSMR NM 88002-5501

DEFNS TECH INFO CTR   1
CENTER DTIC BLS
BLDG 5 CAMERON STATION
ALEXANDRIA
VA 22304-6145

ARMY MISSILE CMND   1
AMSMI
REDSTONE ARSENAL
AL 35898-5243

ARMY DUGWAY PROVING GRD   1
STEDP 3
DUGWAY UT 84022-5000

USATRADOC   1
ATCD FA
FT MONROE VA 23651-5170

ARMY FIELD ARTLRY SCHOOL   1
ATSF
FT SILL OK 73503-5600

WSMR TECH LIBRARY BR   1
STEWS IM IT
WSMR NM 88001

Record Copy   32

TOTAL   116